p24 mAb according to the manufacturer's protocol. The percentage of infected cells on day 40 was 90.6% in U937/N2 cells, whereas in U937/TLMA-15 and U937/TLMA-18 cells, these values remained at only 10.2% and 17.0%, respectively (Fig. 2A). By day 48, the percentage of infected U937/N2 cells was 95.4%, whereas U937/TLMA-15 and U937/TLMA-18 cells remained at 16.4% and 16.6%, respectively (Fig. 2B).

Detection of HIV-1 DNA using PCR

TLMA2993 transfected cells were mixed with 0.5 ml of the culture supernatant of HIV-1 IIIB infected U937 cells and incubated for 1 h at 37 °C in a CO_2 incubator with shaking. After incubation, cells were collected at 24 and 48 h. The amount of HIV-1 DNA detected by PCR at 24 and 48 h after HIV-1 infection was significantly suppressed in U937/TLMA-15 and U937/TLMA-18 while that of U937/N2 was at an appreciable level (Fig. 3).

Discussion

Since TLMA2993 significantly inhibited reverse transcription in a cell free system [1], we designed, and synthesized an artificial cDNA to generate TLMA2993 in the transfectants. As expected, the transfectants became resistant to HIV-1 infection. The amount of TLMA2993 peptide detected by competitive ELISA was 1.8 μM for U937/TLMA-15 and 1.3 μM for U937/TLMA-18, and U937/TLMA-15 showed a higher resistance than U937/TLMA-18 (Figs. 2 and 3). It is clear that the data shown in Figs. 2 and 3 reflected the results of competitive ELISA. Since the levels of expression of CD4, CCR5, and CXCR4 were essentially the same among the cells, resistance could be correlated with the amount of TLMA2993 expressed and was dose dependent.

Inhibition of HIV-1 infection in the transfectants was actually due to suppression of RT function, since generation of HIV-1 DNA at an early stage of infection was suppressed (Fig. 3). It is likely that the current dose of nucleoside analogues or non-nucleoside drugs could be lowered by combination with TLMA2993 peptide or other complementary peptides of RT. A stronger effect on HIV-1 infection would be expected if the three kinds of complementary peptides were combined. It will be necessary to also test peptides similar to TLMA2993 such as PSTW1954 and ESLA2340 that are other RT inhibitors [1], and to confirm their effects in the cell. Complementary peptides of RT will have a potential to cure HIV-1 infected patients and this complementary peptide anti-viral therapy provides a novel approach.

The method described here may be applicable to the regulation of any intracellular functional protein. Complementary peptides such as TLMA2993 can be designed using a program such as MIMETIC, and these may be expressed using an artificial cDNA as a means of regulating target molecules in cells.

Acknowledgments

We thank Dr. William Campbell and Dr. Eliada Lazoura for English editing of the manuscript and valuable comments. We also thank Dr. Jun-ichi Miyazaki for providing pCXN2 expression vector. This work was supported by a research grant from the Organization for Pharmaceutical Safety and Research and by Grants-in-Aid from the Ministry of Education, Science, Sports and Culture, Japan.

References

[1] W. Campbell, L. Kleiman, L. Baranyi, Z. Li, A. Khorchid, E. Fujita, N. Okada, H. Okada, A novel genetic algorithm for designing mimetic peptides that interfere with the function of a target molecule, Microbiol. Immunol. 46 (2002) 211–215.

[2] T. Grundstrom, W.M. Zenke, M. Wintzerith, H.W. Matthes, A. Staub, P. Chambon, Oligonucleotide-directed mutagenesis by microscale 'shot-gun' gene synthesis, Nucleic Acids Res. 13 (1985) 3305–3316.

[3] G. Safrany, N. Tanaka, T. Kishimoto, Y. Ishikawa, H. Kato, R. Kominami, M. Muramatsu, Structural determinant of the species-specific transcription of the mouse rRNA gene promoter, Mol. Cell. Biol. 9 (1989) 349–353.

[4] H. Niwa, K. Yamamura, J. Miyazaki, Efficient selection for high-expression transfectants with a novel eukaryotic vector, Gene 108 (1991) 193–200.

[5] L. Faulkner, M. Patel, P.M. Brickell, D.R. Kats, The role of the Fgr tyrosine kinase in the control of the adhesive properties of U937 monoblastoid cells and their derivetives, Immunology 92 (1997) 519–526.

[6] R. Ohta, M. Imai, Y. Fukuoka, T. Miwa, N. Okada, H. Okada, Characterization of mouse DAF on transfectant cells using monoclonal antibodies which recognize different epitopes, Microbiol. Immunol. 43 (1999) 1045–1056.

[7] H. Okada, X. Wu, N. Okada, Complement-mediated cytolysis and azidothymidine are synergistic in HIV-1 suppression, Int. Immunol. 10 (1998) 91–95.

[8] X. Wu, N. Okada, H. Momota, R.F. Irie, H. Okada, Complement-mediated anti-HIV-1 effect induced by human IgM monoclonal antibody against ganglioside GM2, J. Immunol. 162 (1999) 533–539.

[9] M. Imai, N. Okada, H. Okada, Inhibition of HIV-1 infection by an intramolecular antisense peptide to T20 in gp160, Microbiol. Immunol. 44 (2000) 205–212.

[10] T.W. Chun, L. Carruth, D. Finzi, X. Shen, J.A. DiGiuseppe, H. Taylor, M. Hermankova, K. Chadwick, J. Margolick, T.C. Quinn, Y.H. Kuo, R. Brookmeyer, M.A. Zeiger, P. Barditch-Crovo, R.F. Siliciano, Quantification of latent tissue reservoirs and total body viral load in HIV-1 infection, Nature 387 (1997) 183–188.

[11] S. Nakajima-Iijima, H. Hamada, P. Reddy, T. Kakunaga, Molecular structure of the human cytoplasmic β-actin gene: Interspecies homology of sequences in the introns, Proc. Natl. Acad. Sci. USA 82 (1985) 6133–6137.

Microbiol. Immunol., 48(10), 767–772, 2004

Delayed HIV-1 Infection of CD4$^+$ T Lymphocytes from Therapy-Naïve Patients Demonstrated by Quantification of HIV-1 DNA Copy Numbers

Kaoru Wada, Hiromi Nagai, Tomoko Hagiwara, Shiro Ibe, Makoto Utsumi, and Tsuguhiro Kaneda*

Clinical Research Center, National Hospital Organization Nagoya Medical Center (Tokai Area Central Hospital for AIDS Treatment and Research), Nagoya, Aichi 460–0001, Japan

Received February 25, 2004; in revised form, June 29, 2004. Accepted July 5, 2004

***Abstract*: Measuring the amount of HIV-1 DNA in infected cells is important to estimate the size of the viral reservoir in patients. However, the clinical impact of the intracellular viral DNA level remains unclear. The present study examines the clinical significance of the HIV-1 DNA level in peripheral CD4$^+$ T lymphocytes from 21 therapy-naïve patients. HIV-1 DNA levels in purified peripheral CD4$^+$ T lymphocytes were measured by the real-time PCR method using the Roche LightCycler system that can detect 200 copies/10^6 cells. We detected intracellular HIV-1 DNA in 15 (71.4%) of 21 patients at levels ranging from 270 to 98,120 copies/10^6 CD4$^+$ cells, with a median of 2,220 copies/10^6 cells. We also found HIV-1 DNA that was below the detection limit in the remaining 6 patients, although 8,800–150,000 copies/ml of HIV-1 RNA were detected in plasma. Circular HIV-1 DNA was not detected in 5 of 6 cases, suggesting that reverse transcription in CD4$^+$ T lymphocytes of these cases was not active. Thus, delayed HIV-1 infection of CD4$^+$ T lymphocytes was demonstrated in these patients. The level of HIV-1 DNA in peripheral CD4$^+$ T lymphocytes indicates the clinical status of therapy-naïve patients.**

***Key words*: Delayed HIV-1 infection, Therapy-naïve, Real-time PCR, HIV-1 DNA**

Human immunodeficiency virus type 1 (HIV-1) efficiently and continuously replicates itself after inserting its genome into the DNA of host cells. Such active viral replication correlates directly with disease progression and patient survival (11). Therefore, the HIV-1 RNA level in plasma directly reflects viral replication and has become a powerful prognostic tool (14).

Highly active antiretroviral therapy (HAART) that basically includes combinations of nucleoside or non-nucleoside inhibitors of reverse transcriptase (RT) and a protease inhibitor(s) can significantly reduce plasma HIV-1 RNA to below detectable levels. However, even after years of HAART treatment, cells harboring replication-competent HIV-1 can still persist in the blood and lymphoid tissues (3–5, 8, 9, 18, 19). This persistent reservoir of infected cells is the major impediment to HIV-1 eradication. Therefore, it is important to estimate the viral reservoir and to study its dynamics by measuring intracellular HIV-1 DNA levels. However, the clinical significance of intracellular HIV-1 DNA levels remains unclear.

Real-time PCR can treat many samples in a short period, making it useful for studying intracellular HIV-1 persistence (6, 7). In this report, we first validated the real-time PCR method and then successively measured intracellular HIV-1 DNA levels in 21 therapy-naïve patients. We specifically aimed to determine the status of HIV-1 infection in patients carrying a detectable plasma viral load, but whose CD4$^+$ T lymphocytes were minimally infected.

Materials and Methods

Patients. Twenty-one therapy-naïve HIV-1-infected patients who underwent initial consultation at Nagoya Medical Center, Japan, were enrolled in this study. The

**Address correspondence to* Dr. Tsuguhiro Kaneda, Clinical Research Center, National Hospital Organization Nagoya Medical Center (Tokai Area Central Hospital for AIDS Treatment and Research), Sannomaru 4–1–1, Naka-ku, Nagoya, Aichi 460–0001, Japan. Fax: +81–52–955–1878, E-mail: kanedat@nnh.hosp.go.jp

Abbreviations: β2M, β_2-microglobulin; HAART, highly active antiretroviral therapy; HIV-1, human immunodeficiency virus type 1; RT, reverse transcriptase.

quantification of HIV-1 was performed after informed consent was obtained.

Measurements of plasma viral load and CD4 cell counts. Viral load was measured using an Amplicor HIV-1 monitor v1.5 system (Roche Diagnostics, Tokyo). CD4 cell counts were performed by flow cytometry with FACSCalibur (Becton Dickinson, Tokyo) using anti-CD4 antibody (DakoCytomation, Kyoto, Japan).

Purification of CD4-positive lymphocytes and DNA extraction. $CD4^+$ lymphocytes were isolated by StemSep column chromatography (Stem Cell Technologies, Vancouver, BC, Canada). Collected cells were washed and resuspended in phosphate-buffered saline. DNA was extracted using QIAamp DNA Blood Kits (QIAGEN, Tokyo).

Preparation of HIV-1 DNA and β2M DNA assay standards. A standard HIV-1 plasmid (pUC-IIIB) was constructed by cloning one copy of HIV-1 IIIB without LTR into pUC118 (TaKaRa, Shiga, Japan). A human β_2-microglobulin (β2M) standard plasmid (pGEM-β2M) was constructed by cloning one copy of β2M exon 2 to pGEM-T (Invitrogen, Tokyo).

Quantification of HIV-1 DNA by real-time PCR. We designed PCR primers and a *Taq*Man probe for HIV-1 DNA based on the HIV-1 subtype B consensus sequence (database of Los Alamos National Laboratory). The amplification primers were located in the *gag* region: forward primer (Gag 1), 5′-CAAGCAGCCATGCAAATGTT-3′ and reverse primer (Gag 2), 5′-GCATGCACTGGATGCAATCT-3′. The *Taq*Man probe has the sequence 5′-FAM-TCCATTCTGCAGCTTCCTCATTGATG-TAMRA-3′. Copy numbers of the β2M gene were determined using the primers, 5′-CAGCAAGGACTGGTCTTTCTATCTCT-3′ and 5′-ACCCCACTTAACTATCTTGG-3′, with the *Taq*Man probe, 5′-FAM-CACTGAAAAAGATGAGTATGCCTGCCGTGT-TAMRA-3′.

Real-time PCR proceeded using an LC Fast Start DNA master mix hybridization probe kit (Roche Diagnostics). The PCR mixtures contained 60 ng of DNA extracts, 2 μl of DNA master mix, 5 mM $MgCl_2$, primers (500 nM each) and the *Taq*Man probe (400 nM) in a total volume of 20 μl. Cycling parameters consisted of denaturation for 10 min at 95 C followed by 45 cycles of 10 sec at 95 C and 30 sec at 60 C. The automated LightCycler system performed the amplification, as well as data acquisition and analysis.

Determination of HIV-1 subtypes and tropisms. We determined the nucleotide sequence of the *V3* region of the *env* gene to classify the HIV-1 subtype and tropism as described (10, 17).

Sequencing HIV-1 gag *region.* Nucleotides containing the region amplified by real-time PCR were amplified by nested PCR using the external primers gag03 (5′-AAAACATATAGTATGGGCAA-3′) and gag05 (5′-GGGCTATACATTCTTACTAT-3′) and the internal primers gag06 (5′-GATAGAGGTAAAAGACACCAA-3′) and gag04 (5′-TAGGTGGATTGTTTGTCATC-3′).

The DNA in both reactions was denatured for 5 min at 95 C followed by 30 cycles of 30 sec at 95 C, 30 sec at 50 C and 1 min at 72 C and a final extension for 7 min at 72 C. The DNA was amplified in a total volume of 50 μl containing 1× LA *Taq* buffer (TaKaRa), 2.5 mM $MgCl_2$, 0.1 mM each dNTP, 400 nM each primer, and 1 U LA *Taq* DNA polymerase (TaKaRa). Genomic DNA (60 ng) was amplified by the first PCR, and 5 μl of this mixture was applied to the nested reaction.

Both sense and antisense strands of PCR products were sequenced directly using BigDye Terminator Sequencing Kits and an ABI PRISM 310 automatic sequencer (Applied Biosystems, Tokyo).

The sequences of the PCR products were deposited in the DNA Data Bank of Japan (accession numbers AB154280 through AB154297).

Detection of unintegrated circular HIV-1 DNA. Unintegrated circular HIV-1 DNA was amplified by nested PCR using C1R1 (5′-GACCTCAGGTACCTTTAAGA-3′) and C1R2 (5′-GCTTAATACTGACGCTCTCGC-3′) primers in the first reaction, and C3R1 (5′-GGGAGCTTTAGATCTTAGCC-3′) and C3R2 (5′-CCTTCTAGCCTCCGCTAGTC-3′) primers in the nested reaction.

The conditions and PCR mixture components were identical to those used for HIV-1 gag sequencing, except *Taq* DNA polymerase (Roche Diagnostics) was substituted for LA *Taq* polymerase.

Results

Accuracy, Reproducibility and Sensitivity of HIV-1 DNA Quantification Using LightCycler

Table 1 shows the validation data obtained using latently HIV-1-infected ACH2 cells containing one provirus per cell. The interassay CV% was 7.1, 11.7, 50.7 and 71.9 at 10^4, 10^2, 5 and 2 copies, respectively. The accuracy (%) values of the corresponding experiments were 100.4±7.1, 101.2±11.9, 101.2±51.3 and 69.7±50.1, respectively. The intra-assay reproducibility of HIV-1 copy numbers was determined as shown in Table 1. When pUC-IIIB standard plasmids were the HIV-1 DNA source instead of ACH2, the accuracy and reproducibly of HIV-1 DNA measurements were identical (data not shown). These results show that quantification of HIV-1 DNA with LightCycler can be performed with high sensitivity and reproducibility. Data were normalized as copies/10^6 cells by measuring copy

Table 1. Accuracy and reproducibility of real-time PCR assay using LightCycler system

HIV-1 DNA	Intra-assay (n=5)			Interassay (n=15)		
(copies/10^4 cells)	Mean±SD	CV%	Accuracy (%)	Mean±SD	CV%	Accuracy (%)
10,000	9,548±321	5.2	95.5±3.2	10,048±712	7.1	100.4±7.1
1,000	944±48	5.1	94.4±4.8	930±67	7.2	93.0±6.7
100	94±5	4.7	94.0±4.5	101±12	11.7	101.2±11.9
50	49±7	13.0	98.4±4.5	53±7	13.1	106.9±14.0
10	11±1.2	14.0	106.9±12.0	12±3.1	25.9	118.7±30.8
5	4.6±1.8	38.3	91.8±35.2	5.1±2.6	50.7	101.2±51.3
2	1.2±0.5	45.3	58.6±26.6	1.4±1.0	71.9	69.7±50.1

Table 2. HIV-1 DNA level of 21 therapy-naïve HIV-1-infected patients

Patient No.	CD4 cell count (cells/μl)	Plasma HIV-1 RNA (copies/ml)	HIV-1 DNA[a] (copies/10^6 cells)	Detection of circular HIV-1 DNA	Subtype
1	602	1,200	1,070	−	B
2	298	1,600	270	+[c]	B
3	388	8,800	<DL[b]	−	B
4	350	13,000	<DL[b]	−	C
5	292	18,000	<DL[b]	−	B
6	295	20,000	2,440	+[d]	E
7	542	33,000	3,600	−	B
8	329	35,000	<DL[b]	−	B
9	715	44,000	450	+[d]	B
10	281	50,000	10,800	+[d]	B
11	441	54,000	1,440	−	B
12	283	70,000	2,220	+[d]	B
13	330	92,000	300	−	B
14	619	93,000	<DL[b]	−	B
15	116	110,000	15,290	+[d]	B
16	98	120,000	98,120	+[c]	B
17	229	150,000	<DL[b]	+[c]	B
18	527	210,000	1,930	+[d]	B
19	49	210,000	2,870	+[d]	B
20	307	250,000	1,620	+[d]	B
21	21	430,000	33,240	+[d]	B
Median (range)	307 (21–715)	54,000 (1,200–430,000)	2,220 (<DL–98,120)		

[a] Average values of HIV-1 DNA assayed in duplicant.
[b] Below limits of detection.
[c] 1 and 2LTR circular DNA.
[d] 1LTR circular DNA.

numbers of the β2M gene since two β2M copy numbers correspond to one cell. Since 10^4 cells were usually used in one assay, we defined the lower limit of detection as 200 copies/10^6 cells.

Total HIV-1 DNA Copy Numbers in CD4$^+$ T Lymphocytes from Therapy-Naïve Patients

We determined the intracellular HIV-1 DNA in 21 therapy-naïve HIV-1-infected patients. Fifteen (71.4%) of the 21 patients had HIV-1 DNA levels ranging from 270 to 98,120 copies/10^6 CD4$^+$ cells, with a median of 2,220 copies/10^6 cells (Table 2). Amounts of HIV-1 DNA were below the limits of detection in the remaining 6 patients (patients 3, 4, 5, 8, 14 and 17).

The HIV-1 subtypes were B (n=19), C (n=1, patient 4) and E (n=1, patient 6).

Matching of Primers and Taq*Man Probe*

To eliminate the possibility that the low HIV-1 copy number was underestimated because of mismatching, we analyzed the nucleotide sequences of HIV-1 DNA from 6 patients containing the same regions as the primers and the *Taq*Man probe region (Fig. 1). The Gag 1 region corresponding to the forward primer did not contain any mutations in patients 3, 5 and 8 with undetectable levels of HIV-1 DNA. However, we iden-

tified one mutation (C→T) in the center of this region in patients 4, 14 and 17. In the Gag 2 region, all patients had some mutations, however, none of them were located at the 3'-OH end. In the *Taq*Man probe region, we identified no mutations in 4 of 6 patients (4, 8, 14 and 17), and one in the remaining 2 patients (3 and 5). We estimated that these mutations were not critical to the real-time PCR reaction because of their positions. Sequencing the HIV-1 DNA from patients with high levels revealed the same or similar nucleotide mutations. We concluded that the low levels of HIV-1 DNA found in the 6 patients were not false-negative values.

Relationship between Intracellular HIV-1 DNA Levels and CD4⁺ Cell Count or Plasma Viral Load

A negative relationship was observed between intracellular HIV-1 DNA levels and $CD4^+$ cell count (R=0.483). The tendency was the same (P=0.033, Kruskal-Wallis test) when the 21 patients were classified into 3 groups (L, <200; IM, 200–350 and H, >350 cells/μl) (Table 3). On the other hand, a positive relationship between intracellular HIV-1 DNA levels and plasma viral load was observed although the association was quite weak (R=0.287). The Kruskal-Wallis test showed no correlation between them (P=0.125).

Detection of Unintegrated Circular HIV-1 DNA

We further investigated whether T lymphocytes from 6 patients were minimally infected with HIV-1 by detecting circular HIV-1 DNAs that are sensitive markers of early HIV-1 infection (2, 12, 13). Figure 2 shows the results of agarose gel electrophoresis. We detected

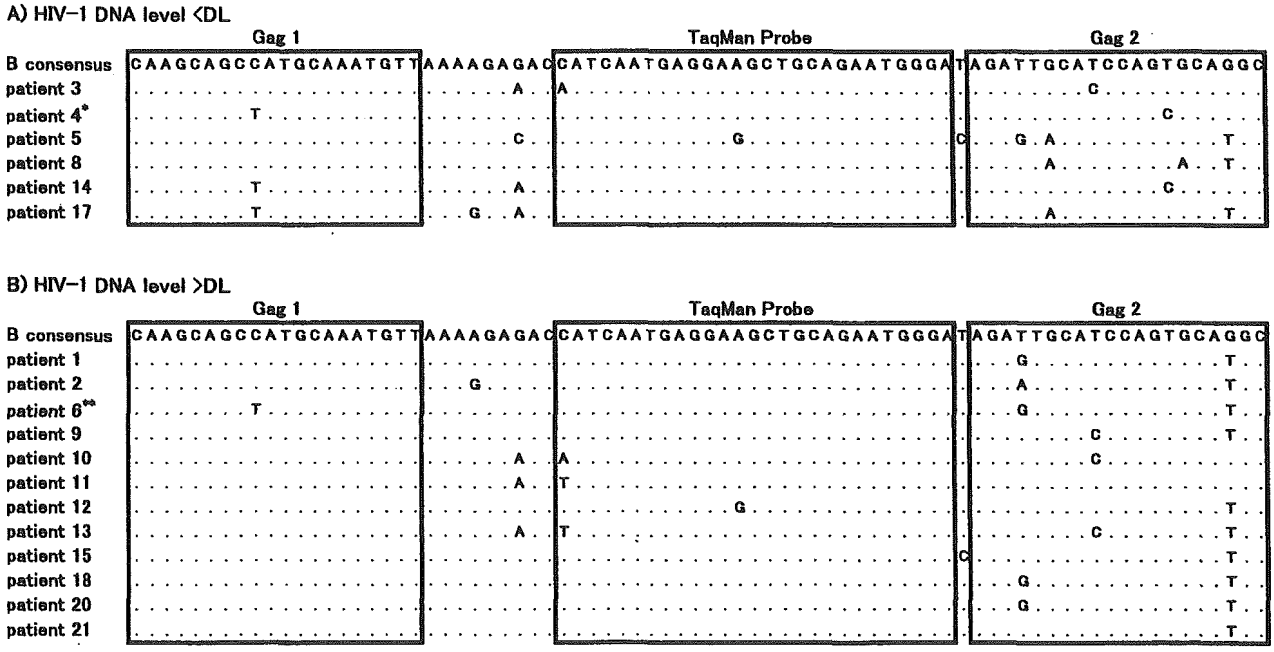

Fig. 1. Nucleotide sequence of amplified region by real-time PCR. Sequences of forward primer (Gag 1), *Taq*Man probe, and reverse primer (Gag 2) used for HIV-1 DNA quantification are boxed. Mutations in these areas are shown by capital letters corresponding to those of mother sequences. *: subtype C, **: subtype E.

Table 3. Levels of HIV-1 DNA according to $CD4^+$ cell count or plasma VL category

Categories	No. of patients tested	HIV-1 DNA (copies/10^6 $CD4^+$ cells)
$CD4^+$ cell count (cells/μl)		
<200	4	24,270 (2,870–98,120)*
200–350	10	1,920 (<DL–10,800)*
>350	7	1,440 (<DL–3,600)*
Plasma HIV-1 RNA (copies/ml)		
<50,000	9	1,070 (<DL–3,600)**
50,000–100,000	5	1,830 (<DL–10,800)**
>100,000	7	9,080 (<DL–98,120)**

*: P=0.033, **: P=0.125 (Kruskal-Wallis test).

one LTR-circular HIV-1 DNA with or without two LTR-circular types in 11 of 15 patients in whom real-time PCR showed that intracellular HIV-1 DNA levels were detectable. However, no circular HIV-1 DNA was detected in the remaining 4 patients who were judged positive by real-time PCR (Table 2). In contrast, as predicted, no circular form HIV-1 DNA was detected among the patients who were judged negative by real-time PCR except patient 17. Circular HIV-1 DNA was detected at a rate of 100% in the group with the highest plasma viral load ($>10^5$ copies/ml), with the lowest $CD4^+$ cell count (<200 cells/μl), and with the highest intracellular HIV-1 DNA levels ($>10^4$ copies/10^6 cells) (Table 4).

Discussion

We measured HIV-1 DNA copy numbers in $CD4^+$ T lymphocytes from 21 therapy-naïve patients using real-time PCR with the Roche LightCycler system. The lower limit of detection was 200 copies/10^6 cells. The intracellular HIV-1 DNA copy numbers ranged from below detectable levels to 98,120 copies/10^6 cells. This distribution was similar to those reported by Désiré et al. (7), Andreoni et al. (1) and Riva et al. (15). Although the number of patients studied might be insufficient to statistically determine an association between plasma HIV-1 viral load and levels of HIV-1 DNA, we identified a weak positive relationship. The key point was the demonstration of the presence of $CD4^+$ T lymphocytes containing a minimal level of HIV-1 DNA in 6 of 21 therapy-naïve patients despite high levels of viral load ranging from 8,800 to150,000 copies/ml. Thereupon, we evaluated the tropism of plasma HIV-1 RNA of these viruses by sequencing the *env V3* region. In all cases, the determined tropism was M-tropic suggesting that viral replication is actively ongoing in target cells of M-tropic HIV-1. In contrast, HIV-1 infection in $CD4^+$ T lymphocytes was not widely established. Current belief is that M-tropic HIV-1 predominantly replicates in patients at the first stage of infection, followed by an increase in T-tropic HIV-1 variants as reported by Schuitemarker et al. (16). According to this model, the very low level of HIV-1 DNA in the $CD4^+$ T lymphocytes found in this study might reflect the infection stage where almost all $CD4^+$ T lymphocytes remain free from HIV-1. Circular HIV-1 DNA was undetectable in most such patients, supporting this notion because this molecular species of HIV-1 DNA reflects active reverse transcription and replication.

From this viewpoint, the HIV-1 DNA copy number in $CD4^+$ T lymphocytes could be a new indicator of the clinical status of HIV-1 infection in therapy-naïve patients. In addition, the delayed HIV-1 infection of $CD4^+$ T lymphocytes could provide new insights into anti-HIV-1 therapy. Selective therapy against M-tropic

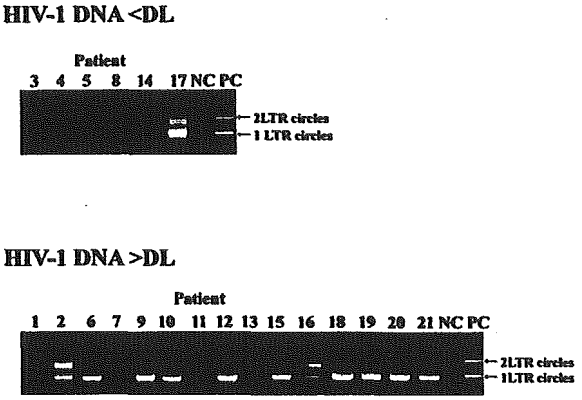

Fig. 2. Detection of unintegrated 1LTR and 2LTR circular HIV-1 DNA in 21 therapy-naïve patients. Molt4 cells were used as negative control (NC) and Molt4-IIIB cells persistently infected with HIV-1 IIIB were used as positive control (PC). Products of PCR electrophoresed in 1% agarose gels were visualized by staining with ethidium bromide.

Table 4. Detection rate of circular HIV-1 DNA in therapy-naïve patients classified as three categories

Categories	Detection rate of circular HIV-1 DNA
$CD4^+$ cell count (cells/μl)	
<200	4/4 (100%)
200–350	6/10 (60%)
>350	2/7 (28.6%)
Plasma HIV-1 RNA (copies/ml)	
<50,000	3/9 (33.3%)
50,000–100,000	2/5 (40.0%)
>100,000	7/7 (100%)
Intracellular HIV-1 DNA (copies/10^6 cells)	
<DL	1/6 (16.7%)
200–10,000	7/11 (63.6%)
>10,000	4/4 (100%)

HIV-1 might retard HIV-1 infection of $CD4^+$ T lymphocytes, delaying or preventing subsequent formation of a lymphocytic HIV-1 reservoir.

This study was partly supported by Health Science Research Grants for HIV/AIDS (H15-AIDS-015 to TK) and Grants for Collaborative Study of National Hospitals for AIDS Treatment (Pub12-2 and Pub14-1 to TK). K. Wada was and H. Nagai is a research resident of the Japanese Foundation for AIDS Prevention.

References

1) Andreoni, M., Parisi, S.G., Sarmati, L., Nicastri, E., Ercoli, L., Mancino, G., Sotgiu, G., Mannazzu, M., Trevenzoli, M., Tridente, G., Concia, E., and Aceti, A. 2000. Cellular proviral HIV-DNA decline and viral isolation in naïve subjects with <5000 copies/ml of HIV-RNA and >500×10⁶/l CD4 cells treated with highly active antiretroviral therapy. AIDS **14**: 23–29.
2) Brusswl, A., Mathez, D., Broche-Pierre, S., Lancar, R., Calvez, T., Sonigo, P., and Leibowitch, J. 2003. Longitudinal monitoring of 2-long terminal repeat circles in peripheral blood mononuclear cells from patients with chronic HIV-1 infection. AIDS **17**: 645–652.
3) Chun, T.W., Carruth, L., Finzi, D., Shen, X., DiGiuseppe, J.A., Taylor, H., Hermankova, M., Chadwick, K., Margolick, J., Quinn, T.C., Kuo, Y.H., Brookmeyer, R., Zeiger, M.A., Barditch-Crovo, P., and Siliciano, R.F. 1997. Quantification of latent tissue reservoirs and total body viral load in HIV-1 infection. Nature **287**: 183–188.
4) Chun, T.W., Stuyver, L., Mizell, S.B., Ehler, L.A., Mican, J.A.M., Baseler, M., Lloyd, A.L., Nowak, M.A., and Fauci, A.S. 1997. Presence of an inducible HIV-1 latent reservoir during highly active antiretroviral therapy. Proc. Natl. Acad. Sci. U.S.A. **94**: 13193–13197.
5) Cone, R.W., Gowland, P., Opravil, M., Grob, P., Ledergerber, B., and the Swiss HIV Cohort Study. 1998. Levels of HIV-infected peripheral blood cells remain stable throughout the natural history of HIV-1 infection. AIDS **12**: 2253–2260.
6) Damond, F., Descamps, D., Farfara, I., Telles, J.N., Puyeo, S., Campa, P., Leprêtre, A., Matheron, S., Brun-Vezinet, F., and Simon, F. 2001. Quantification of proviral load of human immunodeficiency virus type 2 subtypes A and B using real-time PCR. J. Clin. Microbiol. **39**: 4264–4268.
7) Désiré, N., Dehée, A., Schneider, V., Jacomet, C., Goujon, C., Girard, P.M., Rozenbaum, W., and Nicolas, J.C. 2001. Quantification of human immunodeficiency virus type 1 proviral load by a TaqMan real-time PCR assay. J. Clin. Microbiol. **39**: 1303–1310.
8) Finzi, D., Blankson, J., Siliciano, J.D., Margolick, J.B., Chadwick, K., Pierson, T., Smith, K., Lisziewicz, J., Lori, F., Flexner, C., Quinn, T.C., Chaisson, R.E., Rosenberg, E., Walker, B., Gange, S., Gallant, J., and Siliciano, R.F. 1999. Latent infection of $CD4^+$ T cells provides a mechanism for lifelong persistence of HIV-1, even in patients on effective combination therapy. Nat. Med. **5**: 512–517.
9) Finzi, D., Hermankova, M., Pierson, T., Carruth, L.M., Buck, C., Chaisson, T.E., Quinn, T.C., Chadwick, K., Margolick, J., Brookmeyer, R., Gallant, J., Markowitz, M., Ho, D.D., Richman, D.D., and Siliciano, R. 1997. Identification of a reservoir for HIV-1 in patients on highly active antiretroviral therapy. Science **278**: 1295–1300.
10) Leitner, T., Korber, K., Robertson, D., Gao, F., and Hahn, B. 1997. Updated proposal of reference sequences of HIV-1 genetic subtype, p.III-19–24. *In* Korber, B., Hahn, B., Foley, B., Mellors, J.W., Leitner, T., Myers, G., McCutchan, F., and Kuiken, C.L. (eds), Human retroviruses and AIDS 1997, Theoretical Biology and Biophysics Group, Los Alamos National Laboratory, Los Alamos, N. Mex.
11) Mellors, J.W., Rinaldo, C.R., Jr., Gupta, P., White, R.M., Todd, J.A., and Kingsley, L.A. 1996. Prognosis in HIV-1 infection predicted by the quantity of virus in plasma. Science **272**: 1167–1170.
12) Nandi, J.S. 1999. Unintegrated viral DNA as marker for human immunodeficiency virus 1 infection *in vivo* and *in vitro*. Acta Virol. **43**: 367–372.
13) Nicholson, W.J., Shepherd, A.J., and Aw, D.W.J. 1996. Detection of unintegrated HIV type 1 DNA in cell culture and clinical peripheral blood mononuclear cell samples: correlation to diseases stage. AIDS Res. Hum. Retrovir. **12**: 315–323.
14) Piatak, M., Saag, M.S., Yang, L.C., Clark, S.J., Kappes, J.C., Luk, K.C., Hahn, B.H., Shaw, G.M., and Lifson, J.D. 1993. High levels of HIV-1 in plasma during all stages of infection determined by competitive PCR. Science **259**: 1749–1754.
15) Riva, E., Antonelli, G., Scagnolari, C., Pistello, M., Capobianchi, M.R., Monforte, A.D., Pezzotti, P., and Dianzani, F. 2003. Human immunodeficiency virus (HIV) DNA load and level of immunosuppression in treatment-naïve HIV-1-infected patients. J. Infect. Dis. **187**: 1826–1828.
16) Schuitemaker, H., Koot, M., Kootstra, N.A., Dercksen, M.W., De Goede, R.E.Y., Van Steenwijk, R.P., Lange, J.M.A., Eeftink Schattenkerk, J.K.M., Miedema, F., and Tersmette, M. 1992. Biological phenotype of human immunodeficiency virus type 1 clones at different stages of infection: progression of disease is associated with a shift from monocytotropic to T-cell-tropic virus populations. J. Vir. **66**: 1354–1360.
17) Shioda, T., Levy, J.A., and Cheng-Mayer, C. 1992. Small amino acid changes in the V3 hypervariable region of gp120 can affect the T-cell-line and macrophage tropism of human immunodeficiency virus type 1. Proc. Natl. Acad. Sci. U.S.A. **89**: 9434–9438.
18) Wong, J.K., Günthard, H.F., Havlir, D.V., Zhang, Z.Q., Haase, A.T., Ignacio, C.C., Kwork, S., Emini, E., and Richman, D.D. 1997. Reduction of HIV-1 in blood and lymph nodes following potent antiretroviral therapy and the virologic correlates of treatment failure. Proc. Natl. Acad. Sci. U.S.A. **94**: 12574–12579.
19) Wong, J.K., Hezareh, M., Günthard, H.F., Havlir, D.V., Ignacio, C.C., Spina, C.A., and Richman, D.D. 1997. Recovery of replication-competent HIV despite prolonged suppression of plasma viremia. Science **278**: 1291–1295.

Inactivation of C5a Anaphylatoxin by a Peptide That Is Complementary to a Region of C5a[1]

Emiko Fujita,* Imre Farkas,*‡ William Campbell,† Lajos Baranyi,† Hidechika Okada,† and Noriko Okada[2]*

PL37 (RAARISLGPRCIKAFTE) is an antisense homology box peptide composed of aa 37–53 of C5a-anaphylatoxin and is considered to be the region essential for C5a function. Using a computer program, we designed the complementary peptides ASGAPAPGPAGPLRPMF (Pep-A) and ASTAPARAGLPRLPKFF (Pep-B). Pep-A bound to PL37 and to C5a with very slow dissociation as determined by analysis using surface plasmon resonance, whereas Pep-B failed to bind at all. C5a was inactivated by concentrations of 7 nM or more of Pep-A, and this concentration of Pep-A inhibited induction of intracellular Ca^{2+} influx in neutrophils. Patch clamp electrophysiology experiments also showed the effectiveness of Pep-A in C5aR-expressing neuroblastoma cells. Furthermore, Pep-A administration prevented rats from C5a-mediated rapid lethal shock induced by an Ab to a membrane inhibitor of complement after LPS sensitization. *The Journal of Immunology,* **2004, 172: 6382–6387.**

Complement anaphylatoxin C5a is a 74-aa peptide generated from the fifth component of complement (C5) during complement activation (1, 2). C5a acts efficiently as an anaphylatoxin, stimulating cells such as leukocytes and endothelial cells, and is also a potent chemotactic factor for neutrophils and other inflammatory cells bearing C5aR. Therefore, C5a is considered to be one of the most potent inflammatory mediators (3). Inflammatory cells respond to nanomolar concentrations of C5a with intracellular calcium mobilization, stimulation of chemotaxis, aggregation, degranulation, and production of superoxide anions (4). Some inhibitors such as peptide or nonpeptide C5a receptor antagonists and anti-C5a Ab have already been reported. However, the design of low molecular mass agents that directly inactivate C5a has been a challenging problem (4).

Peptide RAARISLGPRCIKAFTE (PL37)[3] is a complement C5a anaphylatoxin fragment (aa 37–53) and is an antisense homology box (AHB) peptide of C5a (5, 6). The sequences within the AHBs were based on the molecular recognition theory, which states that peptides that are encoded on opposite strands of DNA in a given reading frame show affinity in binding each other and that this binding occurs as a result of the hydropathic complementary of the peptides. In addition, such sense-antisense amino acid sequences might represent both intra- and intermolecular interaction sites. Approximately 8- to 15-aa-long regions of this type were found in proteins, which we termed AHBs (5). PL37 is an AHB of C5a; however, it is also antisense to two regions of the C5aR (6). PL37 in multiple antigenic peptide form (PL37-MAP) evoked inward calcium current pulses on human neuroblastoma TGW cells or dibutyryl cAMP-treated U937 cells (6, 7). Therefore, we generated complementary peptides (C-peptides) to PL37, expecting that they could interfere with the function of C5a. To design the C-peptides, we used the software program MIMETIC (8). The algorithm scores several physicochemical parameters of each candidate peptide. C-peptides generated in this manner have already been shown to be inhibitory to HIV-1 reverse transcriptase (8) and thrombomodulin (9).

We synthesized two C-peptides targeting PL-37, and examined their reactivity to PL37-MAP and C5a in various assays such as binding measurements, intracellular calcium mobilization, calcium influx, and in an in vivo C5a-mediated lethal shock rat model (10–12).

Materials and Methods

Design of C-peptides

We used the evolutionary software program MIMETIC (Institute for Protein Science. Nagoya, Japan) to design C-peptide sequences for interaction with PL37 (7). MIMETIC assigns a score using a genetic algorithm based on several physicochemical parameters including hydropathic complementarity optimization, average structural similarity optimization, minimization of bulky side chain interference, and backbone alignment. MIMETIC uses a genetic algorithm that generates a series of peptides by random alteration and by shuffling segments to optimize fitting to the target. MIMETIC then ranks the C-peptides according to their score. We synthesized the two highest score peptides and tested their activity.

Measurement of binding interactions by surface plasmon resonance (SPR)

Binding interactions between PL37 or C5a with C-peptides were evaluated using SPR technology with the Biacore system (Biacore International, Upsala, Sweden). PL37 and C5a were covalently immobilized on the CM5 sensor chip by amine-coupling methods using *N*-ethyl-*N*-(dimethylaminopropyl)carbodiimide/*N*-hydroxysuccinimide (EDC/NHS) according to the manufacturer's instructions. We activated the surface of the CM5 sensor

*Department of Biodefense, Nagoya City University Graduate School of Medical Sciences, Nagoya, Japan; †Choju Medical Institute, Fukushimura Hospital, Toyohashi, Japan; and ‡Department of Endocrine Neurobiology, Institute of Experimental Medicine, Hungarian Academy of Science, Budapest, Hungary

Received for publication November 18, 2003. Accepted for publication March 15, 2004.

The costs of publication of this article were defrayed in part by the payment of page charges. This article must therefore be hereby marked *advertisement* in accordance with 18 U.S.C. Section 1734 solely to indicate this fact.

[1] This work was supported in part by a Grant for Research on Specific Diseases of the Ministry of Health, Labour and Welfare, Japan. I.F. was supported by the fellowship program of the Japanese Society for the Promotion of Science.

[2] Address correspondence and reprint requests to Dr. Noriko Okada, Department of Biodefense, Nagoya City University Graduate School of Medical Sciences, Mizuho-cho, Nagoya 467-8601, Japan. E-mail address: drnoriko@med.nagoya-cu.ac.jp

[3] Abbreviations used in this paper: AHB, antisense homology box; P37, peptide RAARISLGPRCIKAFTE; PL37-MAP, PL37 in multiple antigenic peptide form; C-peptide, complementary peptide; SPR, surface plasmon resonance; EDC/NHS, *N*-ethyl-*N*-(dimethylaminopropyl)carbodiimide/*N*-hydroxysuccinimide; EA, ethanolamine hydrochloride; RU, units of resonance response; Pep-A, Peptide A (ASGAPAPGPAGPLRPMF); Pep-B, Peptide B (ASTAPARAGLPRLPKFF).

0022-1767/04/$02.00

chip with EDC/NHS for 20 min before injection with PL37-MAP (200 μg/ml in 10 mM sodium carbonate buffer, pH 8.5, over flow cell 2) or C5a (100 μg/ml in 10 mM acetate buffer, pH 5, over flow cell 3). Afterward, excess NHS was deactivated for 20 min with 1 M ethanolamine hydrochloride (EA), pH 8.5. The reference flow cell was activated with EDC/NHS and blocked with EA. Coupling was performed at a flow rate of 5 μl/min at 25°C in PBS. Analyte (30 μl of C-peptide A or B) was injected at 10 μl/min at 25°C in PBS. Binding interactions were determined by passing samples simultaneously over both the EA-blocked cell and the flow cell with immobilized PL37 or C5a so as to obtain units of resonance response (RU) by subtraction of the background using Biacore software (BIA evaluation).

Patch clamp measurements

The measurements were conducted on TGW human neuroblastoma cells bearing C5aR. Cells were voltage clamped at room temperature at a holding potential of −70 mV using a whole cell clamp configuration. The instruments used for electrophysiology were an Axopatch 200-A patch clamp amplifier, a Digidata-1200 data acquisition system; and pCLAMP 6.02 software from Axon Instruments (Foster City, CA). The head stage of the amplifier was fitted to an MHW-3 hydraulic manipulator manufactured by Narishige (Tokyo, Japan), and the cells were visualized using an Olympus IMT-2 invert microscope (Olympus, Melville, NY). Data acquisition and analysis were performed using an IBM-compatible personal computer. Patch electrodes (OD = 1.5 mm; thin wall; Garner Glass, Claremont, CA) were pulled with a PP-83 puller and polished with an MF-83 microforge (Narishige). The resistance of patch electrodes was 8–10 MΩ. The solutions used were as follows: an extracellular solution (10 mM HEPES, 140 mM NaCl, 5 mM KCl, 2 mM $CaCl_2$, 2 mM $MgCl_2$, 10 mM glucose, pH 7.34); and an intracellular pipette solution (10 mM HEPES, 110 mM KCl, 15 mM NaCl, 0.1 mM $CaCl_2$, 2 mM $MgCl_2$, 1 mM EGTA, pH 7.25). Recordings were conducted on several cells (n = 10 in each experiment) and were initiated simultaneously with the peptide application.

The PL37-MAP peptide or mixture of peptides (PL37-MAP and C-peptides) were incubated in an Eppendorf tube at room temperature for 1 h in the extracellular solution and then applied to the cells via a puff pipette from a distance of 300–500 μm for 2 min.

Neutrophil isolation

Neutrophils were isolated from fresh human blood with 0.2% EDTA as an anticoagulant. Whole blood was collected from a healthy volunteer (a collaborator of this study) via venipuncture. A 2.4-ml aliquot of blood was then layered onto 2 ml of Mono-Poly Resolving Medium (Dainihon Seiyaku, Tokyo, Japan) in a centrifuge tube and centrifuged at 400 × g for 20 min at room temperature. The polymorphonuclear leukocytes (neutrophils) were then harvested, and the cell fraction was washed with HBSS.

Intracellular Ca^{2+} mobilization measurement

The isolated neutrophils were loaded with 2 μM fura-2/AM (Molecular Probes, Eugene, OR) mixed with 0.02% Pluronic F-127 (Molecular Probes) and 0.2% DMSO in HBSS for 40 min at 37°C. The suspension was agitated to prevent sedimentation. After loading, the cells were washed with HBSS twice and suspended in HBSS containing 0.3% BSA (HBSS/BSA). Approximately 1 × 10^6 cells in 900 μl of HBSS/BSA were added to a poly-L-lysine-coated 35-mm petri dish and allowed to attach to the bottom of the dish for 30 min. Changes in intracellular calcium concentrations in response to C5a or a mixture of peptides (C-peptides and C5a) were determined by monitoring the ratio of fluorescence light emission at 510 nm as a result of excitation at 340 and 380 nm at 37°C using an ARGUS HiSCA calcium imaging system (Hamamatsu Photonics, Hamamatsu, Japan). The mixture of peptides and C5a was incubated in an Eppendorf tube on ice for 30 min in the HBSS solution and then applied to the cells after a 2-min baseline recording.

Rat lethal shock induced by anti-Crry Ab after LPS priming

Administration of anti-rat Crry mAb (5I2) (10) induces lethal shock in rats primed with a trace amount of LPS (11, 12). With this model, all rats sensitized with 0.05 mg/kg LPS died within 30 min of injection of mAb 5I2.

Male Wistar rats weighing ~250 g were purchased from Chubu Kagaku Shizai (Nagoya, Japan) and were allowed free access to food and water. Each rat was injected with 0.05 mg/kg LPS, prepared from a phenol extraction of *Salmonella typhosa* (Sigma-Aldrich, St. Louis, MO) in 250 μl of saline. After 20 h, 0.75 mg/kg 5I2 was administered. Ten minutes before the injection of 5I2, saline or C-peptides in saline were injected. All injections were administered i.v. through the tail vein. Animal experiments were conducted according to the Nagoya City University Guideline for the Care and Use of Experimental Animals and approved by the Nagoya City University Graduate School of Medical Sciences Animal Care Committee.

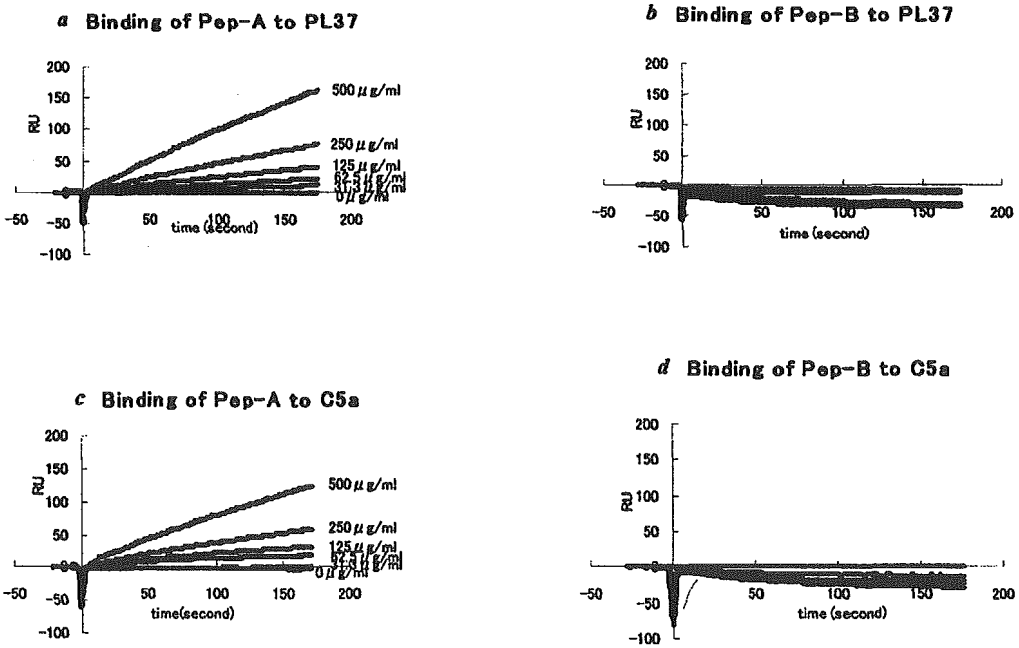

FIGURE 1. Binding of C-peptides to immobilized PL37-MAP and C5a using Biacore equipment. An overlay plot of response curves was obtained from the Biacore instrument when various concentrations of Pep-A and Pep-B were injected. All samples were injected at time 0, and the association was monitored as an increase in RU. *a*, Various concentrations of Pep-A were injected over the PL37-MAP-coupled flow cell. *b*, The same concentrations of Pep-B were also injected over the PL37-MAP-coupled flow cell. *c*, Pep-A was injected over the C5a-coupled flow cell at the same concentrations of Pep-A as in *a*. *d*, The same concentrations of Pep-B were also injected over the C5a-coupled flow cell.

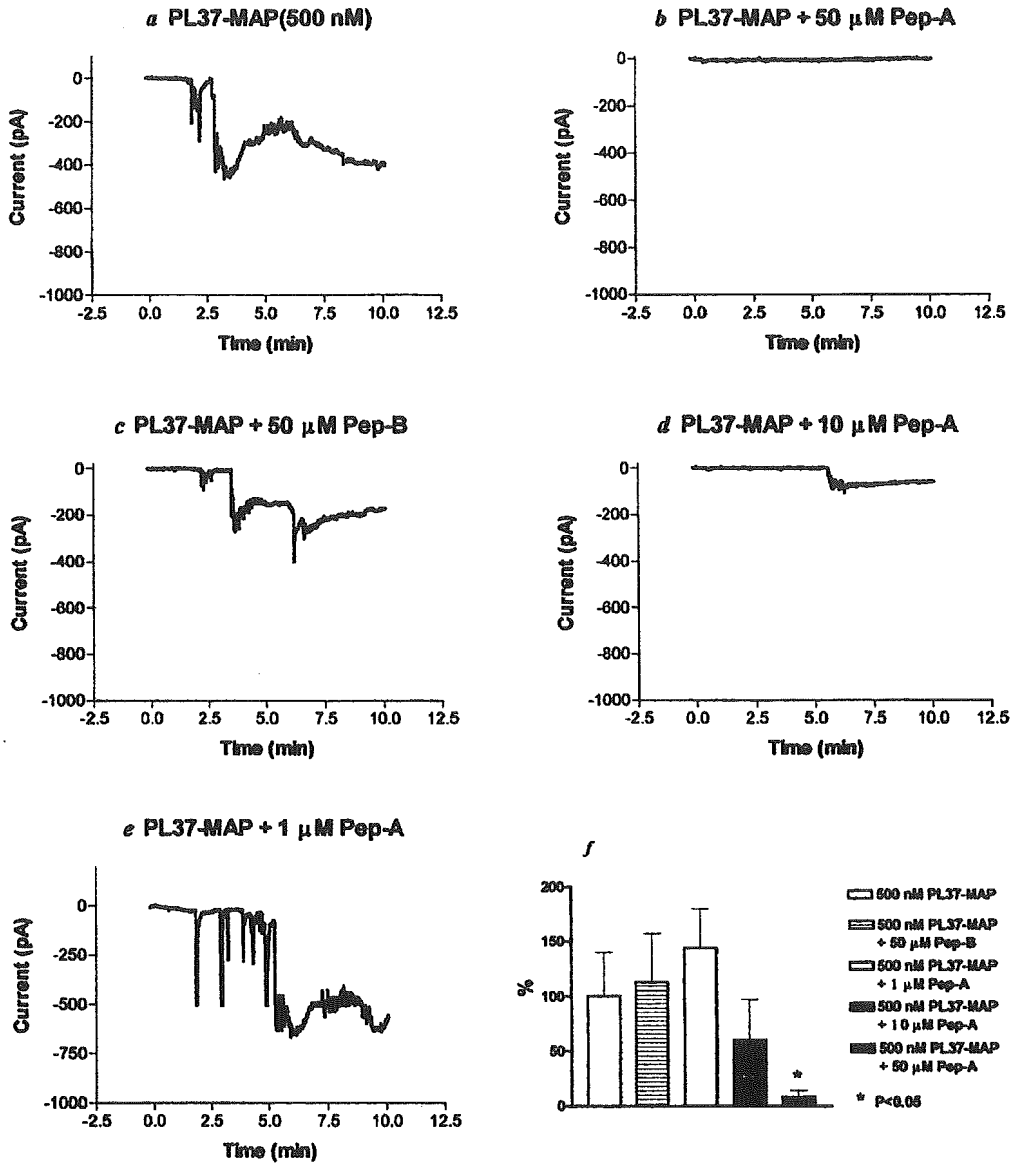

FIGURE 2. Inward ion current pulses of human TGW cells treated with PL37-MAP and C-peptides. *a*, 500 nM PL37-MAP induced inward current pulses with an amplitude of 500 pA. *b*, When the PL37-MAP was mixed and incubated with 50 μM Pep-A, a pulse could not be induced. *c*, 50 μM Pep-B did not have any effect on the ion current evoked by PL37-MAP. d, A lower concentration (10 μM) of Pep-A partially inhibited the ion current triggered by PL37-MAP. *e*, When 1 μM Pep-A was mixed and incubated with PL37-MAP, no inhibition was found. *f*, Concentration dependency of the area-under-curve data. These results show that Pep-A had a significant and concentration-dependent effect on the ion current pulses induced by PL37-MAP.

Results

C-peptides generated to a target peptide, PL37

The best fit peptide sequences to the target region of C5a (sequence of PL37: RAARISLGPRCIKAFTE) designed by MIMETIC were Peptide A (Pep-A: ASGAPAPGPAGPLRPMF) and Peptide-B (Pep-B: ASTAPARAGLPRLPKFF).

Binding of C-peptides to PL37-MAP and C5a

The Biacore instrument that uses SPR technology measures association and dissociation in real time of an unlabeled analyte with an immobilized ligand. PL37-MAP was covalently coupled to a CM5 sensor chip, resulting in a net increase of 8979 RU.

As analytes, Pep-A and Pep-B were injected over the PL37-MAP-coupled flow cell and to the flow cell coupled with EA only. All cycles were performed in PBS at 25°C at a flow rate of 10 μl/min. As shown in Fig. 1*a*, binding data for the PL37-MAP-coupled flow cell were adjusted by subtraction of the data obtained by injection of the same sample over the EA-blocked flow cell (background). Pep-A bound to PL37-MAP, whereas Pep-B did not (Fig. 1, *a* and *b*). Binding of Pep-A was concentration dependent. Pep-A bound to PL37-MAP did not dissociate by increasing the salt concentration or by the addition of DMSO. A 6 M urea treatment was required to dissociate the complex.

Binding of C-peptides to C5a was also examined. C5a was covalently coupled to a CM5 sensor chip resulting in a net increase of 5770 RU. As analytes, Pep-A and Pep-B were injected over both the C5a-coupled and EA-coupled (as the control) flow cells. All cycles were performed in PBS at 25°C at a flow rate of 10 μl/min. In Fig. 1*c*, the binding data for the C5a-coupled flow cell were adjusted by subtraction of the data obtained by injection of

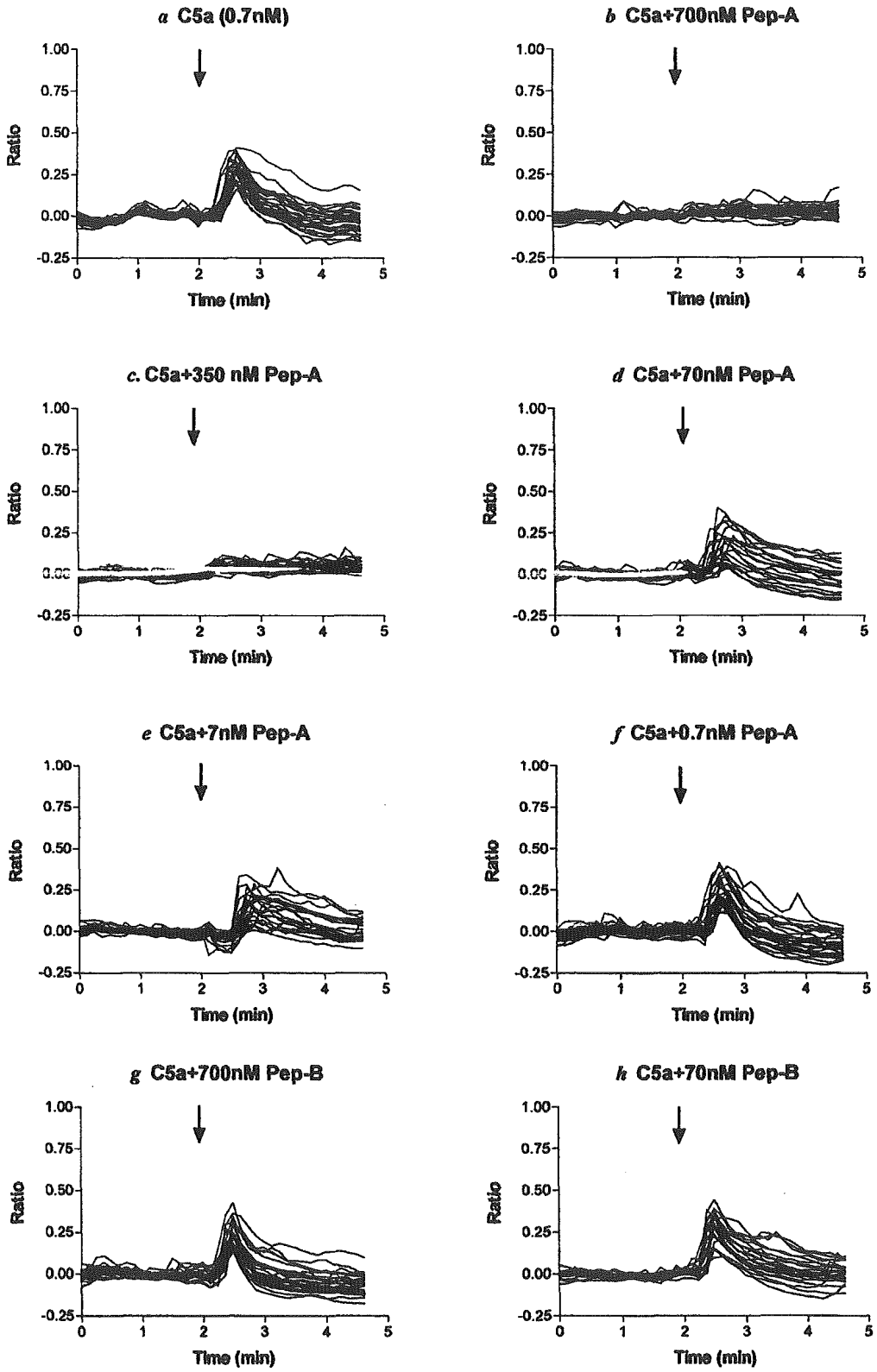

FIGURE 3. Measurement of intracellular Ca^{2+} mobilization in neutrophils using a calcium imaging system *a*, 0.7 nM C5a triggered a transient calcium influx in neutrophils. *b*, Incubation with 700 nM Pep-A blocked the effect of C5a completely. *c*, 95% inhibition was found when 350 nM Pep-A was incubated with C5a. *d* and *e*, Lower concentrations of Pep-A (70 or 7 nM) caused partial inhibition. *f*, The inhibitory effect was not detected when 0.7 nM Pep-A was mixed with C5a. *g* and *h*, Pep-B (700 or 70 nM) failed to cause inhibition of the calcium influx triggered by C5a. The area-under-curve data show the concentration dependency of the inhibitory effect of Pep-A.

the same sample over the EA-blocked flow cell (background). Pep-A bound to C5a, whereas Pep-B did not (Fig. 1*d*). Binding of Pep-A was concentration dependent. Furthermore, no dissociation of Pep-A bound to C5a was observed without treatment with 6 M urea.

Ca^{2+} influx measurement of TGW cells

As reported previously, inward calcium current pulses detected by a patch clamp assay, were evoked when TGW cells were exposed to 500 nM PL37-MAP (Fig. 2*a*). However, 50 μM Pep-A inhibited the pulse almost completely (Fig. 2*b*). After washing out, 500 nM PL37-MAP alone was added to the same cells without incubation with C-peptide, and the PL37-MAP peptide triggered an ion current pulse (data not shown). Pep-B did not block the ion current evoked by PL37-MAP (Fig. 2*c*). Inhibition by Pep-A was concentration dependent, because lower concentrations of the C-peptide blocked the effect of PL37-MAP only partially (Fig. 2, *d* and *e*). When the cells were exposed to Pep-A alone, ion current could not be observed even at the highest concentration used (not shown). Normalized data for amplitudes of the ion current responses are shown in Fig. 2*f*.

Intracellular Ca^{2+} mobilization measurement of neutrophils

The effect of C-peptides on C5a function was analyzed by measuring Ca^{2+} mobilization using an ARUGUS HiSCA calcium imaging system (Hamamatsu, Japan). Administration of 0.7 nM recombinant human C5a induced a transient increase in the level of intracellular Ca^{2+} of human neutrophils (Fig. 3*a*). The level of this activation was ~50% of the maximum achieved with higher concentrations of C5a. A mixture of C-peptide and C5a was incubated in an Eppendorf tube on ice for 30 min in the HBSS solution and then applied to the cells. Incubation of C5a with 700 nM Pep-A inhibited the Ca^{2+} mobilization almost completely (Fig. 3*b*). A lower concentration of Pep-A (350 nM) still inhibited ~95% of the effect of C5a (Fig. 3*c*). Inhibition was therefore concentration dependent: lowering the concentration of Pep-A resulted in a higher amplitude of calcium influx triggered by C5a (Fig. 3, *d* and *e*). The inhibitory effect of Pep-A disappeared at 0.7 nM (Fig. 3*f*). However, incubation of C5a with Pep-B showed no inhibition at any concentration used (700 and 70 nM Pep-B; Fig. 3, *g* and *h*). The results were normalized results using the area-under-curve data of the calcium influx and are described in Fig. 4.

Effect of C-peptides in a rat lethal shock model

Administration of 0.75 mg/kg anti-rat Crry mAb (10) induces rapid lethal shock in rats primed with 0.05 mg/kg LPS 20 h earlier (11, 12). The lethal outcome was C5a mediated (12). To investigate the inhibitory effect of the C-peptides in this model, we injected rats with saline (for the control) or C-peptides in 250 μl of saline 10 min before the 5I2 injection. All rats injected with saline died within 30 min (Table I). However, all rats injected with 4 mg/kg Pep-A survived. The inhibition was concentration dependent.

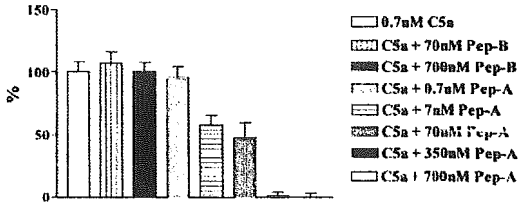

FIGURE 4. The area-under-curve graph of the data of Fig. 3 show the concentration dependency of the inhibitory effect of Pep-A.

Table I. *Effect of C-peptides on the rat lethal shock model*

C-peptides[a]	Surviving/Total No. of Rats	Survival Rate (%)
Saline alone	0/8[b]	0
Pep-B, 4 mg/kg	0/4	0
Pep-A		
4 mg/kg	4/4[b]	100
2 mg/kg	2/3	67
1 mg/kg	1/3	33
0.5 mg/kg	3/4	75

[a] C-peptides in 250 μl of saline were injected i.v. 10 min before the i.v. injection of anti-Crry mAb.

[b] Saline control and Pep-A, 4 mg/kg, are statistically significant ($p < 0.003$, Fisher's method).

Lowering the concentration of Pep-A (from 2 mg/kg to 1 mg/kg) resulted in a lower proportion of surviving rats. Some of the surviving rats stopped breathing briefly in the first 1 or 2 min after injection of 5I2, but were soon breathing again, and ~20 ~ 40 min later began moving. When the LPS-sensitized rats were treated with Pep-A without anti-Crry mAb administration, the animals survived with no harmful effect of Pep-A. In contrast, all rats injected with Ab and 4 mg/kg Pep-B died, as did those treated with the saline control.

Discussion

Various C5aR antagonists have already been reported, and some of these interfered with C5a-mediated functions in vitro and in vivo (3, 13–15). However, the only reported inhibitors of C5a were anti-C5a Abs (16–18). In this study, we designed C-peptides expecting them to interact directly with C5a, resulting in abrogation of C5a function. Two peptides, PepA and PepB, were designed by the computer program MIMETIC to target PL37, an AHB region of human C5a (aa 37–53). Pep-A bound to the target PL37, as determined using SPR technology, and inhibited the inward ion current pulse induced by PL37-MAP in neuroblastoma cells and C5a induction of intracellular Ca^{2+} mobilization in neutrophils. Furthermore, Pep-A bound to the whole C5a molecule so strongly that the complex could be dissociated only with 6 M urea.

Although Pep-B was designed by the same method as used for Pep-A and although both Pep-A and Pep-B showed maximum best fit values using MIMETIC, Pep-B showed no reactivity with PL37-MAP or C5a in any assay conducted. Careful examination of Pep-A and Pep-B might therefore provide useful information for improvement of the algorithm. Furthermore, the information obtained will contribute to a better understanding of peptide characteristics necessary to ensure interaction with a target amino acid sequence.

Two binding sites in C5a to C5aR have been reported. One is at the core of C5a and is centered around Arg 40 (19). The other is contained in the eight amino acids of the C terminus (20). PL37 is located around the first binding site. Pep-A was designed against the PL37 sequence of C5a and inhibited the function of both C5a and PL37. Therefore, our data demonstrate that this AHB-derived PL37 is an important region in C5a.

Treatment with Pep-A was effective in our rat lethal shock model. In this model, rats primed with LPS died within 30 min when injected with anti-Crry mAb. In addition, the lethal outcome was mediated by C5a (12). Hence, our data suggest that Pep-A might bind selectively to C5a in vivo. However, one weak point of using peptide drugs is their short half-life in vivo. Therefore, a time delay between triggering shock and administration of the peptide could be crucial. Administration of 4 mg/kg Pep-A 30 min before the injection of anti-Crry mAb was not effective, indicating

that PeP-A had been degraded in 30 min in vivo. The variable results at lower concentration of Pep-A (Table I) could be due to the short half-life of the peptide in vivo. In contrast, this short half-life could be advantageous. In endotoxic shock, endotoxin induces transient activation of complement and generation of C5a and C3a fragments, which cause lethal shock. In this form of shock, the short duration of the peptide drug and its rapid clearance would be an advantage in avoiding possible long-lasting side effects. Indeed, rats injected with Pep-A survived without any noticeable deleterious side effects.

Acknowledgments

We thank Dr. Akemi Hayakawa of Nagoya University School of Medicine for her help in analysis with SPR technology. We thank Catherine Campbell for English editing of the manuscript.

References

1. Ember, J. A., and T. E. Hugli. 1997. Complement factors and their receptors. *Immunopharmacology 38:3.*
2. Gerard, C., and N. P. Gerard. 1994. C5a anaphylatoxin and its seven transmembrane-segment receptor. *Annu. Rev. Immunol. 12:775.*
3. Sumichika, H., K. Sakata, S., Takeshita, S. Ishibuchi, M. Nakamura, T. Kamahori, S. Ehara, K. Itoh, T. Ohtsuka, T. Ohbora, et al. 2002. Identification of a potent and orally active non-peptide C5a receptor antagonist. *J. Biol. Chem. 277:49403.*
4. Michael, K. 2001. Targeting complement in therapy. *Immunol. Rev. 180:177.*
5. Baranyi, L., W. Campbell, K. Ohshima, S. Fujimoto, M. Boros, and H. Okada. 1995. The antisense homology box: a new motif within proteins that encodes biologically active peptides. *Nat. Med. 1:894.*
6. Baranyi, L., W. Campbell, and H. Okada. 1996. Antisense homology boxes in C5a receptor and C5a anaphylatoxin. *J. Immunol. 157:4591.*
7. Farkas, I., L. Baranyi, Z. S. Liposits, T. Yamamoto, and H. Okada. 1998. Complement C5a anaphylatoxin fragment causes apoptosis in TGW neuroblastoma cells. *Neuroscience 86:903.*
8. Campbell, W., L. Kleiman, L. Baranyi, Z. Li, A. Khorchid, E. Fujita, N. Okada, and H. Okada. 2002. A novel genetic algorithm for designing mimetic peptides that interfere with the function of a target molecule. *Microbiol. Immunol. 46:211.*
9. Shimomura, Y., T. Kawamura, H. Koura, W. Campbell, N. Okada, and H. Okada. 2003. Modulation of procarboxypeptidase R (proCPR) activation by complementary peptides to thrombomodulin. *Microbiol. Immunol. 47:241.*
10. Takizawa, H., N. Okada, and H. Okada. 1994. Complement inhibitor of rat cell membrane resembling mouse Crry/p65. *J. Immunol. 152:3032.*
11. Matsuo, S., S. Ichida, H. Takizawa, N. Okada, L. Baranyi, A. Iguchi, B. P. Morgan, and H. Okada. 1994. In vivo effects of monoclonal antibodies that functionally inhibit complement regulatory proteins in rats. *J. Exp. Med. 180:1619.*
12. Mizuno, M., K. Nishikawa, N. Okada, S. Matsuo, K. Ito, and H. Okada. 1999. Inhibition of a membrane complement regulatory protein by a monoclonal antibody induces acute lethal shock in rats primed with lipopolysaccharide. *J. Immunol. 162:5477.*
13. Konteatis, Z. D., S. J. Siciliano, G. Van Riper, C. J. Molineaux, S. Pandya, P. Fischer, H. Rosen, R. A. Mumford, and M. S. Springer. 1994. Development of C5a receptor antagonists: differential loss of functional responses. *J. Immunol. 153:4200.*
14. Kondo, C., M. Mizuno, K. Nishikawa, Y. Yuzawa, and S. Matsuo. 2001. The role of C5a in the development of thrombotic glomerulonephritis in rats. *Clin. Exp. Immunol. 124:323.*
15. Pellas, T. C., W. Boyar, J. van Oostrum, J. Wasvary, L. R. Fryer, G. Pastor, M. Sills, A. Braunwalder, D. R. Yarwood, R. Kramer, et al. 1998. Novel C5a receptor antagonists regulate neutrophil functions in vitro and in vivo. *J. Immunol. 160:5616.*
16. Stevens, J. H., P. O'Hanley, J. M. Shapiro, F. G. Mihm, P. S. Satoh, J. A. Collins, and T. A. Raffin. 1986. Effects of anti-C5a antibodies on the adult's respiratory distress syndrome in septic primates. *J. Clin. Invest. 77:1812.*
17. Hatherill, J. R., K. E. Stephens K. Nagao, A. Ishizaka, L. Wilmarth, J. C. Wang, T. Deinhart, J. W. Larrick, and T. A. Raffin. 1989. Effects of anti-C5a antibodies on human polymorphonuclear leukocyte function: chemotaxis, chemiluminescence, and lysosomal enzyme release. *J. Biol. Response Mod. 8:614.*
18. Czermak, B. J., V. Sarma, C. L. Pierson, R. L. Warner, M. Huber-Lang, N. M. Bless, H. Schmal, H. P. Friedl, and P. A. Ward. 1999. Protective effects of C5a blockade in sepsis. *Nat. Med. 5:788.*
19. Mollison, K. W., W. Mandecki, E. R. Zuiderweg, T. A. Fey, R. A. Krause, R. G. Conway, L Miller, R. P. Edalji, and M. A. Shallcross. 1989. Identification of receptor-binding residues in the inflammatory complement protein C5a by site-directed mutagenesis. *Proc. Natl. Acad. Sci. USA 86:292.*
20. Kawai, M., D. A. Quincy, B. Lane, K. W. Mollison, J. R. Luly, and G. W. Carter. 1991. Identification and synthesis of a receptor binding site of human anaphylatoxin C5a. *J. Med. Chem. 34:2068.*

FULL PAPER *Virology*

A Potential Live Vector, Foamy Virus, Directed Intra-Cellular Expression of Ovine Interferon-τ Exhibited the Resistance to HIV Infection

Yoichi FUJII[1], Yasunori MURASE[1,5], Kaori OTAKE[2], Yasuko YOKOTA[3], Shinya OMOTO[1], Hidetoshi HAYASHI[1], Hidetika OKADA[4], Noriko OKADA[4], Masahiro KAWAI[4], Harumi OKUYAMA[1] and Kazuhiko IMAKAWA[5]

[1]*Graduate School of Pharmaceutical Sciences, Nagoya City University, Nagoya 467–8603,* [2]*Nagoya University Hospital, Nagoya, 466–8560,* [3]*Department of Immunology, National Institute of Infectious Disease, Tokyo 162–8640,* [4]*Graduate School of Medical Sciences, Nagoya City University, Nagoya 467–8603 and* [5]*Laboratory of Animal Breeding, Graduate School of Agricultural and Life Sciences, The University of Tokyo, Tokyo 113–8657, Japan*

(Received 16 December 2002/Accepted 16 September 2003)

ABSTRACT. Interferon-tau (IFN-τ), produced by the embryonic trophectoderm, is a member of type I IFNs required for the establishment of pregnancy in the ruminant ungulates. Although this IFN possesses antiviral activity similar to other type I IFNs, the effectiveness of IFN-τ as an antiviral agent has not been well characterized. To investigate possible antiviral effects of ovine IFN-τ (oIFN-τ), oIFN-τ–GST fusion protein was expressed in *E. coli* BL21, from which the purified protein isolated possessed anti-viral activity. An apathogenic human foamy virus (hFV) was then used to establish a potential recombinant live vector consisting of oIFN-τ cDNA sense (+) or anti-sense (–) sequence, oIFN-τ(+)/hFV or oIFN-τ(–)/hFV, respectively. Human hematopoietic and other mammalian cell lines that had been transduced with hFV vector consisting of no oIFN-τ, oIFN-τ(+)/hFV or oIFN-τ(–)/hFV construct were cultured initially for 12 days, and three of cell lines were then maintained for up to 90 days. These cells with oIFN-τ expression directed by hFV exhibited the *in vitro* cytopathic effect minimally. Transduced cell lines that had been cultured for 90 days were subjected to studies on human immunodeficiency virus type-1 (HIV-1) infection, which was measured with infectivity of viral particles resulted from the GFP inserted T-cell tropic HIV SF2 or macrophage tropic HIV SF162: the number of HIV-1 positive cells was reduced by the hFV driven-intra-cellular oIFN-τ expression. Since oIFN-τ/hFV transduced cells exhibited the resistance to HIV-1 infection and/or replication, oIFN-τ could be considered as one of effective antiviral agents against HIV-1. These results suggest that the hFV genome could be an effective recombinant live vector for the expression of a targeted gene in various cell types.

KEY WORDS: foamy virus, HIV, interferon-tau, live vector, ovine.

J. Vet. Med. Sci. 66(2): 115–121, 2004

Interferon-tau (IFN-τ) is produced by the embryonic trophectoderm of the ruminant ungulates during the peri-implantation period [1, 12, 16, 18, 25], and the quantity of IFN-τ production appears to be associated with the degree of trophectodermal elongation [12, 17]. Because ovine and bovine IFN-τs attenuate the production of the uterine luteolysin, prostaglandin F2α, and maintain corpus luteum function, these IFN-τs have been regarded as factors essential for the establishment of gestation in these animals. IFN-τ genes are structurally related to those of IFN-α, -β and -ω [3, 4, 15], all of which possess an antiviral activity in a similar manner [23], however, unlike those IFNs, expression of IFN-τ is not induced by viruses or double stranded RNA [9, 28]. Furthermore, interferon regulatory factor (IRF-1), which *trans*-activates IFN-α and -β genes [11], does not regulate IFN-τ gene expression [7].

Effects of ovine IFN-τ (oIFN-τ) on reproductive processes such as the maintenance of corpus luteum function and secretion of uterine proteins are well studied, however, a role that oIFN-τ plays as an antiviral agent has not been carefully characterized. Recently, exogenous oIFN-τ was shown to exhibit anti-feline and anti-human immunodeficiency virus (FIV and HIV) activity *in vitro* [8, 24], which was abrogated by the use of an anti-oIFN-τ antibody [24]. Perhaps more importantly, the antiviral activity exhibited by oIFN-τ did not show much cytotoxic activity, which is usually associated with the use of IFN-α of humans or other mammalian species. These results suggest a possibility that oIFN-τ could be used to block or at least to reduce the degree of viral infection. However, effective transfer of oIFN-τ gene or cDNA into the cells and the subsequent *de novo* synthesis of oIFN-τ against viral infection have not been examined.

Spuma foamy viruses (FVs) have been isolated from a variety of animal species including feline, bovine and humans [14]. Foamy virus is a complex retrovirus with a genomic organization resembling that of a lentivirus such as HIV [10]. The FV genome contains three structural genes (*gag, pol* and *env*) and three auxiliary genes (*bel*-1, -2 and -3). Of these, the transactivator (Tas) encoded by *bel*-1 is essential for viral replication but *bel*-2 and *bel*-3 are not required for viral replication *in vitro*. It has been reported that a foreign reporter gene could be inserted into the *bel*-2 region of FV genome [30]. Furthermore, FV is highly cytopathic when fibroblastic cells are infected with FV *in vitro*, however, FV has been shown to be apathogenic *in vivo*. Because a safe live vector for a gene delivery system remains to be developed, an infectious but apathogenic FV genome could become a candidate vector for the develop-

* CORRESPONDENCE TO: DR. IMAKAWA, K., Laboratory of Animal Breeding, Graduate School of Agricultural and Life Sciences, The University of Tokyo, Tokyo 113–8657, Japan.

ment of such systems.

To investigate whether the human FV (hFV) genome could be a suitable gene delivery system, which would support intra-cellular expression of oIFN-τ, and if oIFN-τ was effective against viral infection, oIFN-τ cDNA was inserted into the *bel*-2 region of the hFV genome. A resulting plasmid, oIFN-τ/hFV construct, was used to transduce human cell lines, which was then examined for its effectiveness against hFV and HIV-1. Here we show that oIFN-τ/hFV minimized HIV's cytopathic effect and viral replication in human monocyte and lymphocyte cell lines.

MATERIALS AND METHODS

Recombinant oIFN-τ and its antibody production: To produce recombinant oIFN-τ protein, the *Nco* I-*Hind* III fragment from the oIFN-τ cDNA plasmid [20] was inserted into the blunted *Bam* H I site of the pGST-4T plasmid (Pharmacia-LKB, Piscataway, NJ, U.S.A.). Upon *E.coli* BL21 cell transformation and expression [17], the recombinant protein was purified with the use of reduced glutathion module (Pharmecia-LKB). Expression of oIFN-τ protein in *E.coli* BL21 was initially determined by using immunoblotting [21] with a rabbit anti-oIFN-τ antibody, kindly provided by Dr. F.W. Bazer (Texas A&M University, U.S.A.). Rabbit anti-oIFN-τ antibody was then prepared by immunization with the recombinant oIFN-τ (100 μg/ml) purified from *E.coli* BL21 lysates in our laboratory [17]; this antibody was used for the remainder of the experiments (Fig. 2, Left panel).

Preparation of oIFN-τ/hFV and HIV-1/GFP constructs: For the preparation of oIFN-τ/hFV construct, the *Sph* I site of the hFV plasmid was digested and filled in with Klenow polymerase. The fragment of oIFN-τ cDNA [15, 20] was obtained by *Eco*R I plus *Hind* III digestions, which was blunt-ended and inserted into the blunted *Sph* I site of the hFV plasmid; hFV vectors containing sense (+) and antisense (–) oIFN-τ cDNA were designated as oIFN-τ (+)/hFV and oIFN-τ (–)/hFV constructs, respectively (Fig. 1A). To construct GFP expression system in a provirus model, T-cell tropic HIV SF2 and macrophage tropic HIV SF162 plasmids were used: These consisted the 5' and 3' half-length subclones of R6/GFP and 9B/R6 (HIV SF2) and R3/GFP and R4 (HIV SF162) containing the *env* and *nef* gene regions in the pUC19 plasmids as described previously [21]. The blunt-ended EGFP fragment that had been isolated with *Nhe* I-*Sal* I digestion from the pEGFP-C1 plasmid (BD Biosciences Clontech, Tokyo, Japan) was inserted into *Sma* I site of pBluescript SK (+) (Stratagene, La Jolla, CA, U.S.A.). After plasmid propagation and the subsequent isolation, the EGFP fragment isolated with *Xho* I digestion was then inserted into *Xho* I sites found in the *nef* portion of the HIV SF2 and HIV SF162 plasmids (Fig. 1B).

Cells and cell transduction with oIFN-τ/hFV construct: Fibroblasts, T-lymphocytes and monocytes were maintained in Dulbecco's modified Eagle's medium supplemented with 10% heat-inactivated fetal bovine serum (FBS) and antibiotics as described previously [13]. Cell types included were hamster kidney fibroblast (BHK-21), feline kidney fibroblast (CRFK), human gingival fibroblast (Gin-1), human T lymphocyte (Molt-4), human T lymphocyte (MT-4), human monocyte (HL-60) and human monocyte (U937). The cells (1×10^5) were each transfected with 2.5 μg of the hFV plasmid, oIFN-τ (+)/hFV or oIFN-τ (–)/hFV construct mixed with 5 μl lipofectin (GIBCO, Rockville, MD, U.S.A.). After transduction with the oIFN-τ construct, the cells were passaged at a 6-day interval and cultured for 12 days or up to three months. On an average of 90 days, the oIFN-τ/hFV transduced cells were then treated with 10^{-6} M trichostatin A (TA) for 24 hr, which had been shown to activate an expression construct in a long term culture [13]. These cells were then subjected to HIV-1/GFP infection

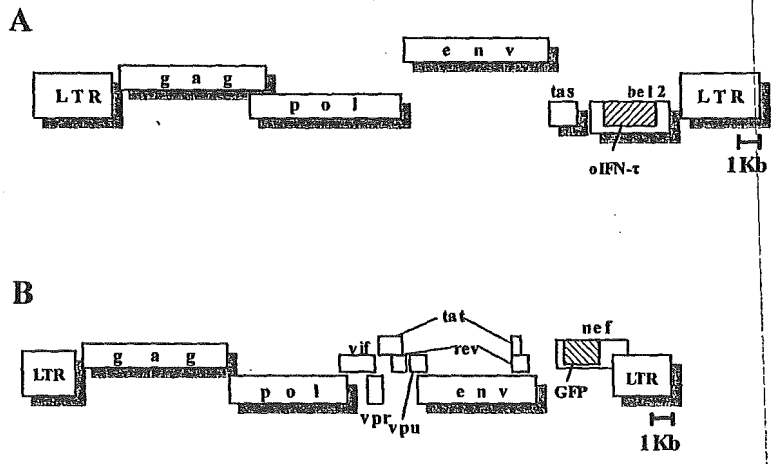

Fig. 1. Schematic representation of oIFN-τ/hFV and HIV/GFP constructs. (A) oIFN-τ cDNA was inserted into the *bel* 2 region of the hFV genome. (B) Construction of recombinant HIV-1/GFP viral vector. GFP sequence was introduced into the *nef* region of HIV-1 SF2 or HIV SF162 strain genomes.

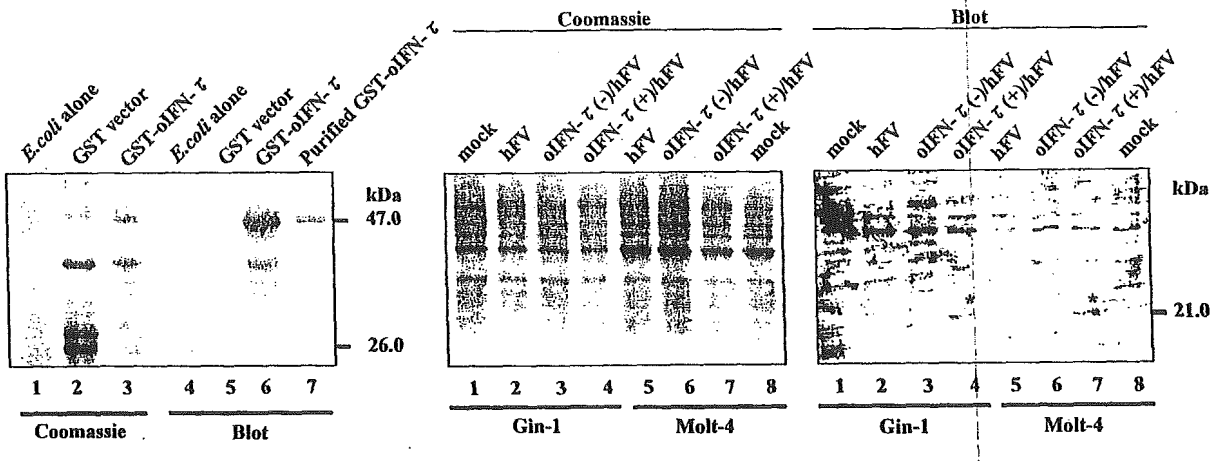

Fig. 2. Expression of recombinant oIFN-τ. Left panel: Lysates from *E. coli* BL21 transformed with the GST-oIFN-τ fusion construct were subjected to SDS-PAGE and Coomassie Blue staining (lanes 1, 2 and 3). Western blot analysis was performed with the use of a rabbit anti-oIFN-τ prepared in our laboratory (lanes 4–7). A purified GST-oIFN-τ is seen as a 47 kDa band. Middle panels: After the treatment with TA for 24 hr, cell lysates from Gin-1 and Molt-4 cells that had been transduced with hFV, oIFN-τ(+)/hFV or oIFN-τ(–)/hFV construct for 90 days were subjected to SDS-PAGE and Coomassie Blue staining. Right panel: Western blot analysis was then performed with the rabbit anti-oIFN-τ. An asterisk indicates a 21 kDa band, resulting from the transduction of Gin-1 or Molt-4 cells with oIFN-τ(+)/hFV construct.

studies. In addition, cell lysates from Gin-1 and Molt-4 cells that had been transduced with mock, hFV, oIFN-τ (+)/hFV or oIFN-τ (–)/hFV construct were also examined for the presence of oIFN-τ after the TA treatment as aforementioned (Fig. 2, Middle and right panels). Due to the anti-proliferative activity exhibited by the members of IFN family, oIFN-τ was also examined for cell growth inhibition activity.

Viral production: Recombinant HIV-1/GFP viruses were generated by the method of Chang-Mayer *et al.* [5]. To generate parental viruses, 2.5 μg of 5' and 3' half-length HIV SF2 or that of HIV SF162 plasmids were transfected into HeLa cells using the lipofectin method as described previously [5]. The cells were cultured at 37°C for 48 hr in 0.5 m*l* of RPMI-1640 medium containing 10% Nu-serum (GIBCO) and antibiotics (complete medium) in a 24-well culture dish. Cell-free supernatants containing viral particles were then collected and used to infect the cells that had been transduced with oIFN-τ/hFV construct (Fig. 3B).

The hFV titer of the culture supernatants was measured by cytopathic effect (CPE) assay as described previously [5]. Briefly, the infected cells were passaged two times at a 6-day interval, and infection was judged by CPE microscopically. The viral titers were measured at 50% tissue culture infective dose ($TCID_{50}$). In a syncytium formation inhibition assay with an infectious clone of hFV, a 50% inhibition rate in the syncytium formation was detected by the use of purified GST-oIFN-τ protein [5]. The presence of hFV DNA with or without oIFN-τ cDNA resulting from cell transduction was also detected by PCR assay. Total DNA was extracted from hFV- or oIFN-τ/hFV-infected cells using the Total DNA Extraction Kit (Stratagene). The presence of oIFN-τ cDNA and/or hFV *gag* DNA in transduced cells was demonstrated by PCR amplification with primers

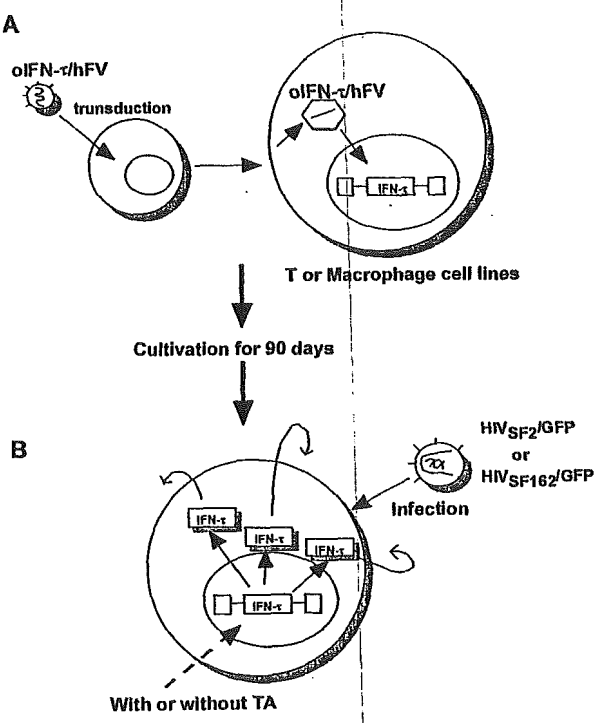

Fig. 3. Establishment of cells transduced with oIFN-τ/hFV, long term cultivation and HIV/GFP infection. (A) Schematic representation of oIFN-τ/hFV transduced cells. T or monocyte cell lines were transduced with the oIFN-τ/hFV construct, and possible integration of oIFN-τ cDNA into the host genome is shown. (B) Working model on the inhibition of HIV-1 infection by oIFN-τ after cultivation for 90 days. Ovine IFN-τ/hFV transduced cells, potentially expressing oIFN-τ, were infected with HIV SF2/GFP or HIV SF162/GFP in the presence or absence of TA.

5'-ccccatggccttcgtgctct-3' and 5'-aggtgagttcagatctccac-3', and primers 5'-tcttacagaccagtaacaa-3' and 5'-gtcaatcattacatctgaca-3', respectively. During culturing of cells transduced with oIFN-τ/hFV, an autocrine effect of oIFN-τ was examined through the determination of viral titer and cell numbers.

For the detection of HIV-1/GFP infection, HeLa cells were fixed with 2.0% paraformaldehyde in PBS, from which the GFP expressed cells were measured by FACS-Calibur and analyzed with Cell Quest (Becton Dickinson, San Jose, CA, U.S.A.) as described previously [21]. Along with GFP-IFN-τ fusion protein, AZT (3'-aziodo-3'-deoxythymidine) and ddI (2', 3'-dideoxyinosine) (Sigma, St. Louis, MO, U.S.A.) were also examined for the prevention of HIV/GFP infection.

RESULTS

The degree of recombinant GST-oIFN-τ fusion protein expression was analyzed by SDS-PAGE with equal protein-equivalents from *E. coli* BL21 cell lysates, followed by Coomassie Blue staining. Immunoblotting was then performed with the rabbit anti-oIFN-τ antibody, and crude and purified GST-oIFN-τ fusion proteins were found as a 47.0 kDa positive band (Fig. 2, left panel).

Virus titers from hFV itself and oIFN-τ/hFV in the culture supernatants were measured by using the CPE assay, and the titers are given as 50% tissue culture infective dose. Seven cell lines, BHK-21, CRFK, Molt-4, MT-4, U937, HL60 and Gin-1, transduced with parental hFV or oIFN-τ (–)/hFV demonstrated CPE after 12 days of *in vitro* culture, whereas the same cell lines transduced with oIFN-τ (+)/hFV exhibited cytopathic effects minimally (Fig. 3A, Table 1). These results indicated that persistent, yet non-cytopathic infection was established with the oIFN-τ/hFV construct *in vitro*. The presence of oIFN-τ and/or hFV DNAs in the transduced cells was then examined using PCR assay with a pair of primers specific for oIFN-τ cDNA and hFV gag genes (Table 1). A 560 bp band specific for a part of the hFV *gag* sequence was found in Molt-4 and Gin-1 cells transduced with hFV (no insert), oIFN-τ (+)/hFV or oIFN-τ (–)/hFV, whereas a 280 bp band specific for oIFN-τ sequence was found in these cells transduced with oIFN-τ (+)/hFV or oIFN-τ (–)/hFV construct (Table 1). Similar results, the presence of a part of hFV *gag* and/or oIFN-τ sequences, were obtained from those of BHK-21, HL60, CRFK, MT-4 and U937 cell lines that had been transduced with hFV, oIFN-τ (+)/hFV or oIFN-τ (–)/hFV construct (Table 1, Fig. 3A). In lysates of Gin-1 and Molt-4 cells that had been transduced with oIFN-τ (+)/hFV, a 21 kDa band, reactive to the oIFN-τ antibody, was found whereas such a band was not detected in the lysates from mock, hFV or oIFN-τ (–)/hFV transduced cells (Fig. 2, right panel)

For the determination of the potential autocrine effect exhibited by oIFN-τ on these cells, an anti-oIFN-τ-antibody was added to the cells transduced with oIFN-τ/hFV construct. The inhibitory activity on virus titer was reduced by 62 ± 3% in the presence of the anti-oIFN-τ-antibody when compared with oIFN-τ/hFV-transduced cells cultured without the antibody. Furthermore, 10^{-4}-diluted culture supernatants from Molt-4 cells that had been transduced with oIFN-τ(+)/hFV construct inhibited approximately 60% of the growth in A375 melanoma cells that are known to express type I IFN receptor [5].

Whereas control GST alone did not inhibit the HIV infection, recombinant oIFN-τ-GST fusion protein, AZT and ddI inhibited the syncytium formation at 20.9 pM (approximately 20 U/m*l*), 70.0 μM and 120.5 μM, respectively. Next, the HIV SF2 (R6/GFP and 9B/R7) or HIV SF162 (R3/GFP and R4) plasmids were transfected into HeLa cells (Fig. 3B), and the degree of transduction with HIV-1/GFP (HIV SF2 or HIV SF162) plasmid was assessed using FACS analysis. Viral particles from the HeLa cell cultures were then introduced to Molt-4, U937 and Gin-1 cells that had been transduced with oIFN-τ/hFV construct for 90 days. Anti-HIV-1 effects of oIFN-τ against HIV SF2 and HIV SF162 recombinant viruses in these cells were then investigated by using syncytium formation inhibition assay [21] and FACS analysis (Table 2). Although HIV-1, HIV SF2 and HIV SF162, infectivity was reduced by the expression of oIFN-τ via oIFN-τ/hFV live vector, the cells that had been transduced with the oIFN-τ (+)/hFV construct inhib-

Table 1. Suppression of cytopathic effects on fibroblasts, T cells and monocytes that had been transduced with hFV live vector consisting of oIFN-τ—cDNA

		CPE assay*				PCR assay**			
Cell line	Origin	No insert	oIFN-τ (+)	oIFN-τ (–)	Mock	No insert	oIFN-τ(+)	oIFN-τ (–)	Mock
BHK-21	Hamster kidney fibroblast	6.5 ± 0.5	< 1.0	4.5 ± 0.3	< 1.0	+/–	+/+	+/+	–/–
CRFK	Feline kidney fibroblast	3.5 ± 0.2	< 1.0	4.4 ± 0.1	< 1.0	+/–	+/+	+/+	–/–
Gin-1	Human gingival fibroblast	2.5 ± 0.8	< 1.0	3.2 ± 0.4	< 1.0	+/–	+/+	+/+	–/–
Molt-4	Human T lymphocyte	4.5 ± 0.8	< 1.0	4.0 ± 0.5	< 1.0	+/–	+/+	+/+	–/–
MT-4	Human T lymphocyte	4.0 ± 0.2	< 1.0	4.2 ± 0.3	< 1.0	+/–	+/+	+/+	–/–
HL-60	Human monocyte	2.0 ± 0.1	< 1.0	2.3 ± 0.2	< 1.0	+/–	+/+	+/+	–/–
U937	Human monocyte	1.2 ± 0.1	< 1.0	2.0 ± 0.1	< 1.0	+/–	+/+	+/+	–/–

Cell lines transduced with sense (+) or antisense (–) oIFN-τ/hFV construct were cultured for 12 days. The culture supernatants were subjected for CPE assay and the cell pellets were simultaneously used for PCR assay. * The values in CPE assay are represented as the mean ± SD of logalithmic 10 $TCID_{50}$/m*l* in triplicate experiments. ** Detections of hFV *gag* DNA/oIFN-τ cDNA, respectively, specific PCR products were performed on agarose gel electrophoresis. +, positve; –, negative.

Table 2. Inhibition of HIV-1 infectivity exhibited by T cells or monocytes that had been transduced with the hFV live vector consisting of oIFN-τ cDNA

Cells	TA	SF2				SF162			
		No insert	oIFN-τ (+)	oIFN-τ (–)	Mock	No insert	oIFN-τ (+)	oIFN-τ (–)	Mock
Molt-4	–	93.6 ± 1.6[a]	49.2 ± 1.4	83.3 ± 3.4	89.4 ± 2.0	79.3 ± 4.0	58.3 ± 2.2	100.0 ± 4.4	85.7 ± 5.0
	+	43.0 ± 3.2	0.7 ± 0.1	45.0 ± 6.5	45.8 ± 1.0	53.3 ± 3.3	0.5 ± 1.4	45.8 ± 8.0	75.2 ± 6.0
U937	–	–[b]	–	–	–	91.4 ± 1.2	25.0 ± 3.5	98.5 ± 5.8	92.8 ± 8.2
	+	–	–	–	–	64.2 ± 2.4	8.5 ± 2.6	62.8 ± 4.2	64.2 ± 3.1
Gin-1	–	1.0 ± 0.1	1.0 ± 0.9	1.0 ± 0.1	1.2 ± 0.2	2.5 ± 0.1	1.7 ± 0.2	1.7 ± 0.5	1.5 ± 0.8
	+	1.2 ± 0.3	0.8 ± 0.2	0.9 ± 1.1	1.1 ± 0.3	1.2 ± 0.1	1.2 ± 0.5	1.2 ± 0.2	1.0 ± 0.2

The sense (+) or antisense (–) oIFN-τ cDNA was introduced via the hFV live vector into Molt-4, U937 or Gin-1cells, which were then cultured for 90 days. HIV-1 SF2/GFP or HIV SF162/GFP was infected to HeLa cells, from which viral particles were obtained and then placed onto the oIFN-τ/hFV transduced cells in the presence (+) or absence (–) TA. The number of GFP positive cells was counted by FACS-Calibur and the percentages of positive cells were analyzed with Cell Quest. [a] Mean ± SD of triplicate experiments. [b] Not tested.

ited approximately 70% of HIV-1 infection after treatment with 10^{-6} M TA for 24 hr (Table 2, Fig. 3B). Following the treatment with TA, however, some non-specific inhibiting activities were found in hFV alone, oIFN-τ(–)/hFV or mock-infected cells (Table 2). Cell transduction with the oIFN-τ/hFV construct was not effective when HIV-1 non-susceptible Gin-1 cells were examined for their infectivity against HIV SF2 or HIV SF162 (Table 2). It should be noted that sufficient inhibition of HIV-1 with oIFN-τ was observed, however, CD4 down-regulation was not recognized in the present investigation.

Because oIFN-τ has been reported to inhibit cell growth [22], the growth of cells transduced with oIFN-τ/hFV construct was then examined. Human FV-transduced Molt-4 and HL60 increased the cell number from approximately 5 × 10^5/m*l* to 9 × 10^5/m*l* and 2.4 × 10^6/m*l* on day 6, and from 5 × 10^5/m*l* to 1.2 × 10^6/m*l* and 1.3 × 10^6/m*l* on day 12, respectively. Numbers of viable Molt-4 and HL60 cells transduced with oIFN-τ/hFV construct also increased from approximately 5 × 10^5/m*l* to 1 × 10^6/m*l* and 1.2 × 10^6/m*l* on day 6, and 1.1 × 10^6/m*l* and 1.3 × 10^6/m*l* on day 12, respectively. On 90 ± 5 days of the culture, however, the growth was inhibited and viabilities of oIFN-τ positive cells were decreased. These data indicated that although oIFN-τ did not affect viable cell numbers in a short-term culture, oIFN-τ reduced the growth rate of oIFN-τ (+) transduced cell lines over the extended period of *in vitro* cultures.

DISCUSSION

Although T-cell and monocyte cell lines transduced with the oIFN-τ/hFV construct rendered resistant to HIV-1 infection, CD4 down-regulation, measured by FACS, was not observed. Possible mechanisms for the inhibition of HIV-1 infection exhibited by oIFN-τ expression include: First, oIFN-τ may have induced some chemokine(s), yet unidentified, expressions on CD4 positive T cell or monocyte cell lines [27], which may then prevent the gp120 binding to chemokine receptors. Second, since another type I IFN such as IFN-β down-regulates a chemokine CCR5 receptor [6], oIFN-τ could also down-regulate cell surface chemokine receptors. Third, oIFN-τ may interfere viral fusion or disrupt integration steps as reported previously [8]. Although a precise mechanism(s) by which HIV-1 replication is prevented awaits further investigations, these data suggest that oIFN-τ could affect several steps of the HIV-1 infection, integration and/or replication cycle in a negative manner.

In contrast to the anti-HIV-1 effect exhibited by oIFN-τ, it is not certain whether a heterologous promoter/enhancer of hFV-LTR was suppressed by oIFN-τ expression or whether replication competent viruses were recovered from the transduced cells. It should be noted that hFV itself has been shown not to induce IFN-α and/or IFN-β in infected cell cultures [30]. Our data, oIFN-τ was expressed by the use of hFV promoter/enhancer system (Fig. 2, right panel), suggest that hFV could be used as a live vector. In addition, the observation that IFN-τ is not induced by a virus or double stranded RNA [9] also suggest that the IFN-τ gene activation could be controlled by a different manner from that of IFN-α and -β [25, 28]. In fact, different promoter/enhancer sequences were found in the IFN-τ genes [20] and specific promoter elements were reported to be essential for the oIFN-τ gene expression [25, 29]. Furthermore, our preliminary experiments provide the evidence that the oIFN-τ enhancer/promoter element was not activated by the trans-activator (Tas) sequence of hFV, and the hFV-LTR was not suppressed by GST-IFN-τ fusion protein expression in human hematopoetic cell lines (Y. Fujii, unpublished observations). Thus, these data indicate that oIFN-τ by itself may not have any effects on hFV replication for a long-term culture in human cell lines.

It has been reported that hIFN-α prevents cell-mediated HIV-1 transmission between lymphocytes and trophoblast *in vitro*, and levels of IFN-α and -β are high in cord blood of HIV-infected women [2, 19]. In women infected with HIV, however, the low vertical transmission rate of HIV to the fetus *in utero* could be due to the protective activity exhibited by placental IFN-α and/or IFN-β. Furthermore, HIV-1 RNA of trans-activating region (TAR) at high concentrations blocks the activation of double-stranded RNA activated protein kinase (PKR) [26], and *Tat* protein functions as decoys of eIF-2, the natural substrate for PKR to evade the IFN response [29]. Nucleotide sequences resemble of IFN-τ genes of the ruminant ungulates have not been found

in the human genome, therefore, the effects and/or therapeutic means by which oIFN-τ may exhibit have not been assessed in a human model. However, the results from the present investigation strongly suggest that the hFV based live vector consisting of oIFN-τ cDNA may be of some values for intervention of infectious diseases in ruminant ungulates and possibly other animal species including humans.

ACKNOWLEDGMENTS. This work was supported in part by a Grant-in-Aid for Scientific Research (13556050) to K. I. from the Japan Society for the Promotion of Science and by the Program for the Promotion of Basic Research Activities for Innovative Bioscience.

REFERENCES

1. Ashworth, C. J. and Bazer, F. W. 1989. Changes in ovine conceptus and endometrial function following asynchronous embryo transfer or administration of progesterone. *Biol. Reprod.* **40**: 425–450.
2. Bake, E., Jimnez, M., Unger, M., Schafer, A., Jauniaux, E. and Vogel, M. 1992. Demonstration of HIV-1 infected cells in human placenta by *in situ* hybridization and immunostaining. *J. Clin. Pathol.* **45**: 871–874.
3. Charlier, M., Hue, D., Boisnard, M., Martal, J. and Gaye, P. 1989. Cloning and expression of cDNA encoding ovine trophoblastin: its identity with a class-II alpha interferon. *Gene* **77**: 341–348.
4. Charlier, M., Hue, D., Boisnard, M., Martal, J. and Gaye, P. 1991. Cloning and structural analysis of two distinct families of ovine interferon-α genes encoding functional class II and trophoblast (OTP) α-interferon. *Mol. Cell Endocrinol.* **76**: 161–171.
5. Cheng-Mayer, C., Quiroga, M., Tung, J.W., Dina, D. and Levy, J.A. 1990. Viral determinants of human immunodeficiency virus type 1 T-cell or macrophage tropism, cytopathogenicity, and CD4 antigen modulation. *J. Virol.* **64**: 4390–4398.
6. Cremer, I., Vieilard, V. and De Maeyer, E. 2000. Retrovirally mediated IFN-beta transduction of macrophages induces resistance to HIV, correlated with up-regulation of RANTES production and down-regulation of C-C chemokine receptor-5 expression. *J. Immunol.* **163**: 1582–1587.
7. Cross, J.C., Werb, Z. and Fisher, S. J. 1994. Implantation and the placenta: key pieces of the development puzzle. *Science* **266**: 1508–1518.
8. Dereuddre-Bosquet, N., Martin, C. M., Mabondzo, A., Gras, F. G., Martal, J. and Dormont, D. 1996. Anti-HIV potential of a new interferon, interferon-τ (trophoblastin). *J. Acquir. Immune Defic. Syndr.* **11**: 241–246.
9. Farin, C. E., Cross, J. C., Tindle, N. A., Murphy, C. N., Farin, P. W. and Roberts, R. M. 1991. Induction of trophoblastic interferon expression in ovine blastocysts after treatment with double-stranded RNA. *J. Interferon Res.* **11**: 151–157.
10. Flugel, R. M. 1992. Spumaviruses: a group of complex retroviruses. *J. Acquir. Immune Defic. Syndr.* **4**: 739–759.
11. Fujita, T., Kimura, Y., Miyamoto, M., Barsoumian, E.L. and Taniguchi, T. 1989. Induction of endogeneous IFN-α and IFN-β genes by a regulatory transcription factor, IRF-1. *Nature (Lond.)* **337**: 270–272.
12. Godkin, J. D., Bazer, F. W., Moffat, J., Sessions, F. and Roberts, R. M. 1982. Purification and properties of a major, low molecular weight protein released by the trophoblast of sheep blastocysts on day 13–21. *J. Reprod. Fertil.* **65**: 141–150.
13. Hatama, S., Otake, K., Ohta, M., Kobayashi, M., Imakawa, K., Ikemoto, A., Okuyama, H., Mochizuki, M., Miyazawa, T., Tohya, Y., Fujii, Y. and Takahashi, E. 2001. Reactivation of feline foamy virus from a chronically-infected feline renal cell line by trichostatin A. *Virology* **283**: 315–323.
14. Hooks, J. J. and Gibbs, C. J. 1975. The foamy viruses. *Bacteriol.Rev.* **39**: 169–185.
15. Imakawa, K., Anthony, R. V., Kazemi, M., Marotti, K. R., Polites, H. G. and Roberts, R. M. 1987. Ovine trophoblast protein-1, a major secretory product of embryonic trophectoderm has sequence similarity to interferons. *Nature (Lond.)* **330**: 377–379.
16. Imakawa, K., Ji, Y., Yamaguchi, H., Tamura, K., Weber, L. W., Sakai, S. and Christenson, R. K. 1998. Co-expression of transforming growth factor β and interferon τ during periimplantation period in the ewe. *Endocr. J.* **45**: 441–450.
17. Klemann, S.W., Li, J., Imakawa, K., Cross. J.C. and Roberts, R.M. 1990. The production, purification and bioactivity of recombinant bovine trophoblast protein-1 (bovine trophoblast interferon). *Mol. Endocrinol.* **4**: 1506–1514.
18. Martal, J., Lacrox, M. C., Loudes, C., Saunier, M. and Wintenberger-Torres, S. 1979. Trophoblastin, an antiluteolytic protein present in early pregnancy in sheep. *J. Reprod. Fertil.* **56**: 63–72.
19. Martin, A. W., Brady, K., Smith, S. I., De Coste, D., Page, D.V., Malpica, A., Wolf, B. and Neiman, R.S. 1992. Immunohistochemical localization of human immunodeficiency virus p24 antigen in placental tissue. *Hum. Pathol.* **23**: 411–414.
20. Nephew, K. P., Whaley, A. E., Christenson, R. K. and Imakawa, K. 1993. Differential expression of distinct mRNAs for ovine trophoblast protein-1 and related sheep type I interferons. *Bio. Reprod.* **48**: 768–778.
21. Otake, K., Fujii, Y., Nakaya, T., Nishino, Y., Zhong, Q., Fujinaga, K., Kameoka, M., Ohki, K. and Ikuta, K. 1994. The carboxyl-terminal region of HIV-1 Nef protein is a cell surface domain that can interact with CD4+ T cells. *J. Immunol.* **153**: 5826–5837.
22. Pontzer, C. H., Bazer, F. W. and Johnson, H. M. 1991. Antiproliferative activity of a pregnancy recognition hormone, ovine trophoblast protein-1. *Cancer Res.* **551**: 5304–5312.
23. Ponzer, C.H, Torres, B., Vallet, J., Bazer, F. and Johnson, H. 1988. Antiviral activity of the pregnancy recognition hormone ovine trophoblast protein-1. *Biochem. Biophys. Res. Commun.* **152**: 801–807.
24. Pontzer, C. H., Yamamoto, J. K., Bazer, F. W., Ott, T. L. and Johnson, H. M. 1997. Potent anti-feline immunodeficiency virus and anti-human immunodeficiency virus effect of IFN-τ. *J. Immunol.* **158**: 4351–4357.
25. Roberts, R. M., Cross, J. C. and Leaman, D. W. 1992. Interferons as hormones of pregnancy. *Endocr. Rev.* **13**: 432–452.
26. Sen, G.C. 2001. Viruses and interferons. *Annu. Rev. Microbiol.* **55**: 255–281.
27. Staggs, K. L., Austin, K. J., Johnson, G. A., Teixeria, M. G., Talbott, C. T., Dooley, V. A. and Hansen, T. R. 1998. Complex induction of bovine uterine proteins by interferon-tau. *Biol. Reprod.* **59**: 293–297.
28. Tan, S.L. and Katze, M.G. 2000. Maneuvering the internetworks of viral neuropathogenesis and evasion of the host defense. *Proc. Natl. Acad. Sci. U.S.A.* **97**: 5684–5686.
29. Yamaguchi, H., Nagaoka, K., Matsuda, F., Xu, N., Christen-

son, R. K., Imakawa, K. and Sakai, S. 2001. Regulation of interferon-τ gene expression and the maternal recognition of pregnancy. *J. Reprod. Develop.* **47**: 69–82.

30. Yu, S. F., Stone, J. and Linial, M. L. 1996. Productive persistent infection of hematopoietic cells by human foamy virus. *J. Virol.* **70**: 1250–1254.